Version 2.0
October 2005

HST Two-Gyro Handbook

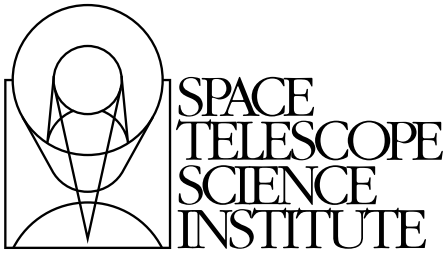

Space Telescope Science Institute
3700 San Martin Drive
Baltimore, Maryland 21218
help@stsci.edu

Operated by the Association of Universities for Research in Astronomy, Inc., for the National Aeronautics and Space Administration

User Support

For prompt answers to any question related to Hubble Space Telescope observations, contact the Space Telescope Science Institute Help Desk at

- **E-mail:** help@stsci.edu
- **Phone:** (410) 338-1082
  (800) 544-8125 (U.S., toll free)

The Space Telescope European Coordinating Facility (ST-ECF) also maintains a Help Desk. European users can contact the ST-ECF for help at

- **E-mail:** stdesk@eso.org

World Wide Web

Information and other resources are available on the HST web site

- **URL:** http://www.stsci.edu/hst

and the HST Two-Gyro Science Mode web site:

- **URL:** http://www.stsci.edu/hst/HST_overview/TwoGyroMode

Proposers are strongly encouraged to check the Two-Gyro Science Mode web site throughout the Cycle 15 Phase I proposal period for updates related to two-gyro operations. Other information, not specific to two-gyro operations, can be accessed through the top-level HST web page above.

Revision History

Version	Date	Editors
2.0	October 2005	Sembach, K.R., et al.
1.0	October 2004	Sembach, K.R., et al.

Citation

In publications, refer to this document as:
Sembach, K. R., et al. 2005, "HST Two-Gyro Handbook", Version 2.0, (Baltimore: STScI)

Send comments or corrections to:
Space Telescope Science Institute
3700 San Martin Drive
Baltimore, Maryland 21218
E-mail:help@stsci.edu

Acknowledgments

The information in this Handbook is a brief summary of the experience gained by many individuals working on the HST two-gyro mode development at STScI and elsewhere. Some of the material contained herein is based upon results of the February 2005 two-gyro on-orbit test, as well as documentation and information available at the HST Two-Gyro Phase I Design Review (February 2004) and Critical Design Review (July 2004). Additional material related to guiding performance and pointing jitter is derived from analyses of HST pointing control simulations performed by the HST Pointing and Control Systems group at Lockheed Martin Technical Operations Company. We thank all of the individuals and groups involved in these design reviews and simulations for their efforts. We especially thank Brian Clapp for his efforts in leading the simulation efforts.

The STScI Two-Gyro Team, which assessed the instrument performance results from the February 2005 tests, includes: Santiago Arribas, Ed Bergeron, Carl Biagetti, John Biretta, Colin Cox, Roelof de Jong, Rodger Doxsey, Ron Gilliland, Anton Koekemoer, Vera Kozhurina-Platais, Ray Lucas, Jennifer Mack, Sangeeta Malhotra, Ed Nelan, Keith Noll, Cheryl Pavlovsky, Adam Riess, Kailash Sahu, Glenn Schneider (U. Arizona), Ken Sembach, Marco Sirianni, Tommy Wiklind, and Chun Xu. The STScI Two-Gyro Planning Team for the February 2005 tests includes Allison Vick, George Chapman, and Merle Reinhart.

Ron Downes provided graphical material and helpful text updates for the observation planning portion of this handbook. We thank Susan Rose and Jim Younger for their assistance with the hardcopy and web-based production of the Handbook.

Table of Contents

Reference Material

CHAPTER 1:

Introduction to Two Gyro-Mode

In this chapter. . .

1.1 Introduction

Just interested in the basic two-gyro information needed to submit your Phase I proposal? Read Chapter 1 and Chapter 2. You can skip the reference material found in later chapters.

The Hubble Space Telescope was originally designed to use three rate-sensing gyroscopes to provide fine pointing control of the observatory during science observations. In order to conserve the lifetime of the HST gyros, one of the functioning gyros was turned off on 28 August 2005 and a new attitude control system that functions with only two gyros was activated. In this mode, two gyros used in combination with the Fine Guidance Sensors provide fine-pointing information during science observations.

The *HST Two-Gyro Handbook* contains information about target visibility and scheduling of HST observations conducted with an attitude

control system relying upon just two gyroscopes. Use the Handbook in conjunction with the appropriate Instrument Handbooks and the *Hubble Space Telescope Call for Proposals* and *Hubble Space Telescope Primer* when assembling your Cycle 15 Phase I proposal. The individual Instrument Handbooks contain detailed technical information about the science instruments and their on-orbit performance. The *Call for Proposals* contains policies and instructions for proposing.

1.2 Two-Gyro Pointing and Jitter

On-orbit tests of the HST two-gyro fine guiding mode and its impact on science instrument performance were carried out on 20-23 February 2005. More than 450 science exposures were obtained with the Advanced Camera for Surveys (ACS), the Near Infrared and Multi-Object Spectrograph (NICMOS), and the Fine Guidance Sensors (FGS) during the three day test. Gyro #1 was removed from the pointing control loop, and Gyros #2 and #4 were used with the FGS to control the HST attitude during all science observations. The attitude control law used during the test was the same as the one that will be used in Cycle 15, with the exception that Gyro #4 will be turned off instead of Gyro #1.

HST fine-pointing performance in two-gyro mode is very similar to the fine-pointing performance observed previously in three-gyro mode.

The HST Pointing and Control Systems group monitored the pointing jitter throughout the two-gyro on-orbit test. For each science exposure, they calculated the jitter at 25 milli-second intervals as estimated by the attitude control law used to maintain the HST pointing. Summaries of the 10-second and 60-second jitter root-mean-square running averages and peak excursions are given in Table 1.1. This table lists the two-gyro 10-second and 60-second mean, median, and maximum jitter values for the sample of 454 exposures. Almost all of the exposures have a mean jitter less than 10 milli-arcseconds. In a few cases, transient pointing disturbances caused small enhancements in the jitter. These types of disturbances are also commonly seen in three-gyro mode (see Chapter 5 for more information about sources of jitter).

Table 1.1: Jitter Measured During the February 2005 Two-Gyro On-Orbit Test

	Jitter (milli-arcseconds, RMS)			
	Avg 10-sec	**Peak 10-sec**	**Avg 60-sec**	**Peak 60-sec**
Two-Gyro Mean	5.6	6.5	6.0	6.2
Two-Gyro Median	5.5	6.2	5.7	6.0
Two-Gyro Maximum	9.5	22.2	10.7	18.0
Percentage of Two-Gyro Exposures with Jitter < 10 mas	100%	97.8%	99.1%	98.7%
Three-Gyro Mean	4.1	5.2	4.2	4.3

Notes: Two-gyro values are based on a sample of 454 exposures taken during the two-gyro on-orbit test (20-23 February 2005). Three-gyro values are based on a sample of 24 exposures taken several days prior to the two-gyro on-orbit test.

The mean two-gyro 60-second-averaged jitter in Table 1.1 is slightly higher than the mean 10-second-averaged jitter because the sample includes several series of short dithered exposures; the 60-second running averages span short periods of slightly increased jitter between exposures as the pointing was changed from one dither position to the next. The jitter values measured during the two-gyro on-orbit test are only slightly larger than those observed in three-gyro mode. The two-gyro values are similar to those predicted by high fidelity simulations conducted in late 2004 and are comparable to those previously available in three-gyro mode (see Chapter 5 and Chapter 6).

There was no loss of fine lock resulting from large pointing disturbances during any of the science observations obtained in two-gyro mode. Loss of lock occurred for 5 of the 36 acquisitions, but these failures have been traced to either bad guide stars or to a minor problem with roll adjustments during the acquisitions at the beginning of the second orbit of several visits. This latter problem was correctable with a minor change to the flight software. The acquisition success rate in two-gyro mode is expected to be >98%.

1.3 Scheduling and Target Visibility

Observations with either orientation or timing constraints may prove more difficult to implement in two-gyro mode than in three-gyro mode because of the additional pointing restrictions necessary for attitude control

and observatory safety. Roughly half the sky is visible at any point in time in two-gyro mode, compared to >80% of the sky in three-gyro mode.

Whenever possible, observers should try to minimize the number of scheduling requirements placed on their observations. This will result in improved schedulability and long range planning, and more efficient use of observing time. Descriptions and examples of how orientation and timing constraints can affect the scheduling of an object and its orbital visibility period can be found in Chapter 2.

Fixed Targets

Observers planning their Cycle 15 Phase I and Phase II proposals should consult Chapter 2, which describes the scheduling of observations in two-gyro mode. The information contained therein has not changed significantly since the initial version of this Handbook was released for Cycle 14. The scheduling information should be used in conjunction with the visibility tools available on the Two-Gyro Science Mode web site and the Visit Planner in the Astronomers Proposal Tools (APT).

Moving Targets

Proposers wanting to observe moving targets should assume that observations in two-gyro mode will work exactly as they did for three-gyro mode, with the caveats that gyro-only tracking and guide star handoffs are not available in two-gyro mode. Moving targets are subject to the same general scheduling and visibility constraints as fixed targets (see Chapter 2). See the *Cycle 15 Call for Proposals* for additional restrictions on moving target observations.

Scheduling Efficiency

At the time this Handbook was being written, the HST Scheduling Group had constructed a long range two-gyro scheduling plan using the Cycle 13 observation pool as a test case to check the scheduling efficiency expected in two-gyro mode. All of the proposals in that cycle were designed for three-gyro mode, so it was necessary to change some of the constraints to make the test proposal pool consistent with implementation under two-gyro mode. The results of the study are an approximation to the scheduling efficiency expected for a fully qualified two-gyro proposal pool. The HST Scheduling Group expects to be able to schedule ~71-73

two-gyro prime orbits per week compared to ~80 prime orbits per week in three-gyro mode. Thus, the scheduling efficiency of HST should remain high in two-gyro mode. Cycle 14 long range planning activities will provide additional information about the expected scheduling efficiency for Cycle 15 and future observing cycles.

1.4 Science Instrument Performance

The science instrument performance during the two-gyro on-orbit test was nearly indistinguishable from the science instrument performance in three-gyro mode. Refer to the appropriate Instrument Handbooks for information regarding the detailed on-orbit performance capabilities of the HST science instruments. Additional information about the performance in two-gyro mode can be found in the Instrument Science Reports listed below.

Instrument Science Reports

Characterization of the ACS/HRC PSF in Two-Gyro Mode, (ACS ISR 2005-11), by M. Sirianni et al.
http://www.stsci.edu/hst/acs/documents/isrs/isr0511.pdf

Two-Gyro Pointing Stability of HST Measured with ACS, (ACS ISR 2005-07), by A. Koekemoer, V. Kozhurina-Platais, A. Riess, M. Sirianni, J. Biretta, & C. Pavlovsky
http://www.stsci.edu/hst/acs/documents/isrs/isr0507.pdf

ACS Coronagraph Performance in Two-Gyro Mode, (ACS ISR 2005-05), by C. Cox & J. Biretta
http://www.stsci.edu/hst/acs/documents/isrs/isr0505.pdf

NICMOS Two-Gyro Mode Coronagraphic Performance, (NICMOS ISR 2005-001), by G. Schneider, A.B. Schultz, S. Malhotra, & I. Dashevsky
http://www.stsci.edu/hst/nicmos/documents/isrs/isr_2005_001.pdf

The FGS Astrometry in the Feb. 2005 On-Orbit Two-Gyro Mode Test, (FGS ISR 2005-01), by E. Nelan
http://www.stsci.edu/HST_overview/TwoGyroMode/documents/FGS.pdf

CHAPTER 2:

Planning Observations in Two-Gyro Mode

2.1 Introduction

Observers will face some changes in the way they design their observing programs in Cycle 15 and future cycles. The conversion to two-gyro operations impacts how observations are scheduled and the visibility periods available for scientific observations. This chapter describes the scheduling constraints encountered during two-gyro operations and provides information necessary for observers to successfully complete their Phase I proposal submissions. The material in this chapter has been distilled from a more extensive discussion of the differences between two-gyro and three-gyro operations found in a previous version of this Handbook (v1.0, Ch. 6)

2.2 All-Sky Availability of Fixed Targets

2.2.1 Overview

The schedulability of an HST observation depends upon many factors and differs considerably between three-gyro and two-gyro operations. To briefly highlight some of these differences, it is useful to compare the accessible regions of the sky in the two modes on a given day of the year.

Figure 2.1: Sky Availability on 5 December 2005

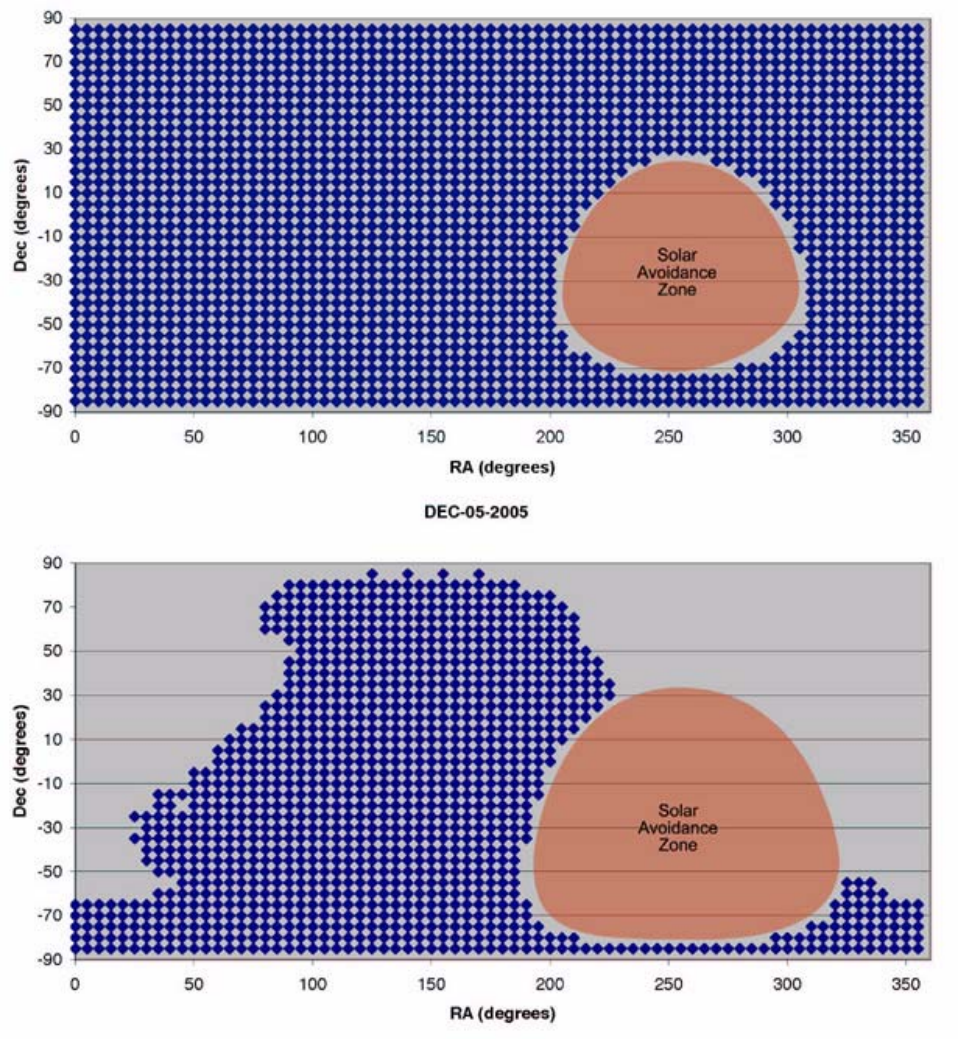

Caption: Sky availability for 5 December 2005 in both three-gyro mode (top panel) and two-gyro mode (bottom panel).

Figure 2.1 shows the sky availability for a single day assuming attitude control with either three gyros (top panel) or two gyros (bottom panel).

Blue regions indicate areas of the sky that can be observed on the date shown, while grey areas of the sky are not observable at that time. The unobservable region of sky is much larger in two-gyro mode than in three-gyro mode because of constraints imposed to achieve guide star acquisitions and to ensure the safety of the observatory. On any given day there is a region of the sky that cannot be observed in either two-gyro or three-gyro mode because of solar avoidance constraints. In three-gyro mode, all regions of the sky outside the solar avoidance zone (50 degree radius) are accessible on any day. The solar avoidance zone for two-gyro mode is larger, with a 60 degree radius. A large region of the sky ahead of the solar avoidance zone (at larger right ascensions than the Sun) is also unobservable in two-gyro mode because of constraints imposed by the process of correcting slew errors and achieving fine guiding lock. Thus, in two-gyro mode most targets can only be observed when they are on the trailing side of the Sun as it moves along the ecliptic. Over the course of the year, all areas of the sky are available in two-gyro mode, but the total time available in any given direction is less than in three-gyro mode.

2.2.2 All-sky Availability Movie

A short narrated movie showing the sky availability during the course of a year can be found on the web at:

http://www.stsci.edu/hst/HST_overview/TwoGyroMode/2GyroMovies/2gyro.html

This movie compares the three-gyro and two-gyro availabilities in one-week increments in a format similar to the figure above. It shows the variable nature of the sky availability in two-gyro mode and the features discussed previously. It also shows that the availability near the equatorial poles is periodic and alternating. This availability pattern at high declinations is tied to the precession of the HST orbit.

2.2.3 Number of Available Days During the Course of a Year

It is useful to consider how many days per year a target of fixed position can be observed by HST. The top panel of Figure 2.2 shows the number of days in a cycle that any position in the sky is observable by HST with three-gyro pointing capabilities. This plot is essentially an encapsulation of the contents of the sky availability movie described above. The color-coding of this figure indicates the number of days for which at least one orbit (defined here to be a contiguous time block of at least 30 minutes) is available to observe a fixed target. In this figure, the allowable Sun angle range is 50-180 degrees. The fewest number of schedulable days occurs over a small swath of sky near the ecliptic, with availability increasing toward the equatorial poles. The minimum number of days available is approximately 260. A large portion of the sky at greater than 50 degrees

ecliptic latitude has at least one schedulable orbit over the entire cycle duration. Be aware that this plot does not convey the information necessary to judge uninterrupted availability as occurs in the continuous viewing zones (CVZs). CVZ opportunities depend on a variety of additional factors that are described elsewhere (see the *HST Primer* and Section 2.6).

Figure 2.2: All-Sky Target Schedulability

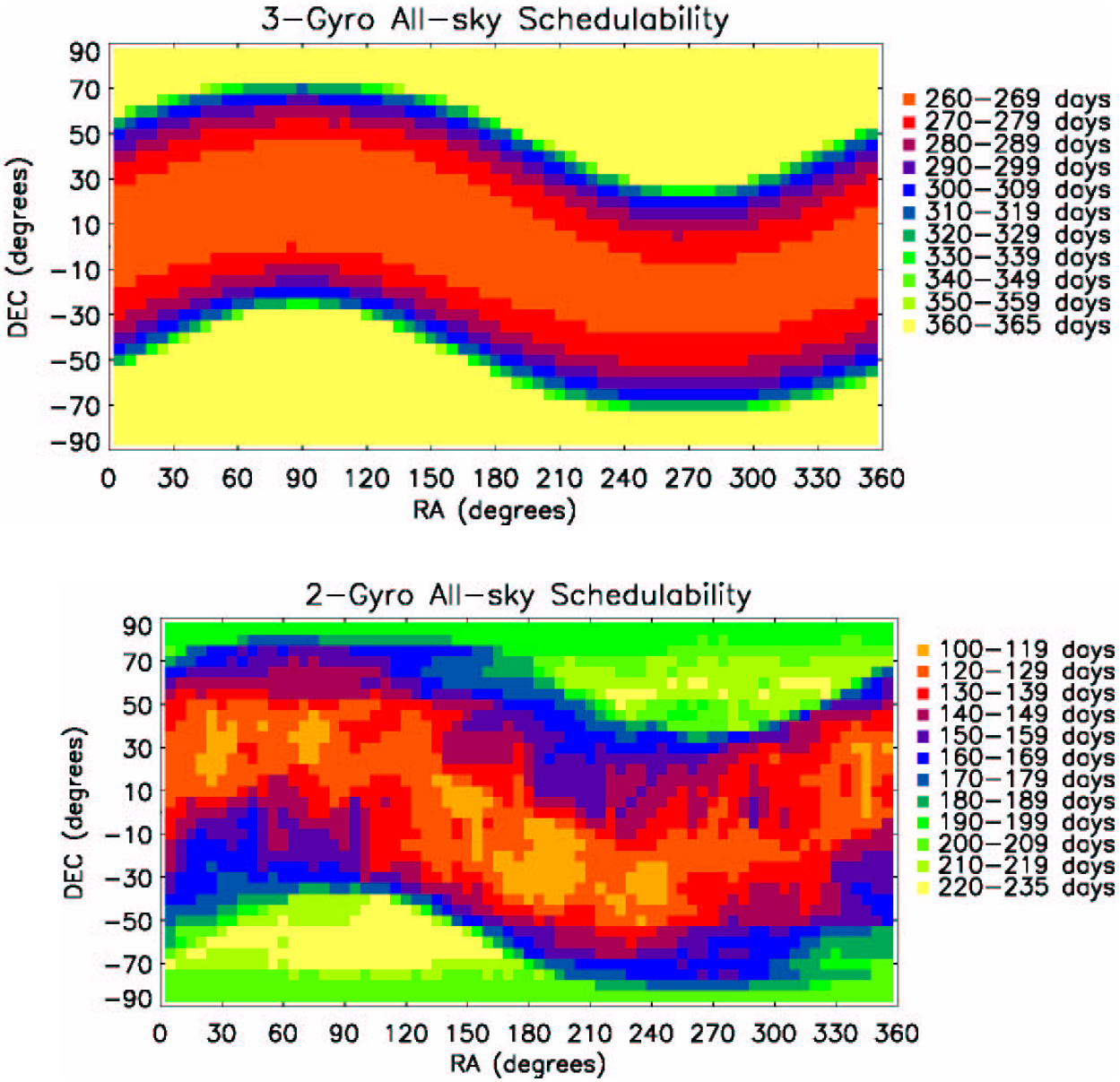

The bottom panel of Figure 2.2 shows the number of days in a cycle that any position in the sky is observable with HST operating in two-gyro mode. Here, the allowable Sun angle range is restricted to 60-180 degrees. Note that the absolute level of the color scaling is different than it is in the three-gyro case shown in the top panel. There are several things worth

noting about this panel when comparing it to the three-gyro results. First, and most importantly, the total number of schedulable days at all positions in the sky decreases substantially in two-gyro mode. Second, the smooth progression in availability seen in the top panel becomes slightly less regular, with pockets of reduced availability occurring across the sky. The overall trend for greater availability increasing toward the equatorial poles remains, but even some high declination pointings have fewer than half as many schedulable days as in three-gyro mode.

2.3 Scheduling Considerations and Visibility Periods for Fixed Targets

2.3.1 Overview

The primary observational constraints on the schedulability of most fixed targets in two-gyro mode are the position of the target in the sky, the required orientation or roll angle of the observatory (if any), and the required timing of the observation (if any). Orientation constraints are usually specified with the `ORIENT` special requirement and often involve a restricted range of allowable roll angles that correspond to a particular time period that HST is able to achieve this orientation. Timing requirements may be specified either implicitly through the `ORIENT` special requirement or explicitly through timing special requirements (e.g., `BETWEEN, AFTER`, etc.). In some cases, an observation may not be schedulable in two-gyro mode because of the restrictions imposed by orientation and/or timing special requirements.

Minimizing the number of special requirements on your observations will improve schedulability.

The operational definition of orbital visibility period for two-gyro operations is the same as it was for three-gyro operations. Orbital visibility is the unocculted time available during the orbit for guide star acquisitions (6 minutes), target acquisitions, science exposures, calibration exposures, and instrument overheads.

Figure 2.3 provides a graphical description of the general decision process involved in determining the schedulability and orbital visibility periods for fixed targets observed in two-gyro mode. The decision process for unconstrained observations involves minimal effort, whereas

constrained observations require more careful consideration of the times of year that an observation can be scheduled. We discuss both types of observations below.

Figure 2.3: Two-Gyro Scheduling and Visibility Decision Tree

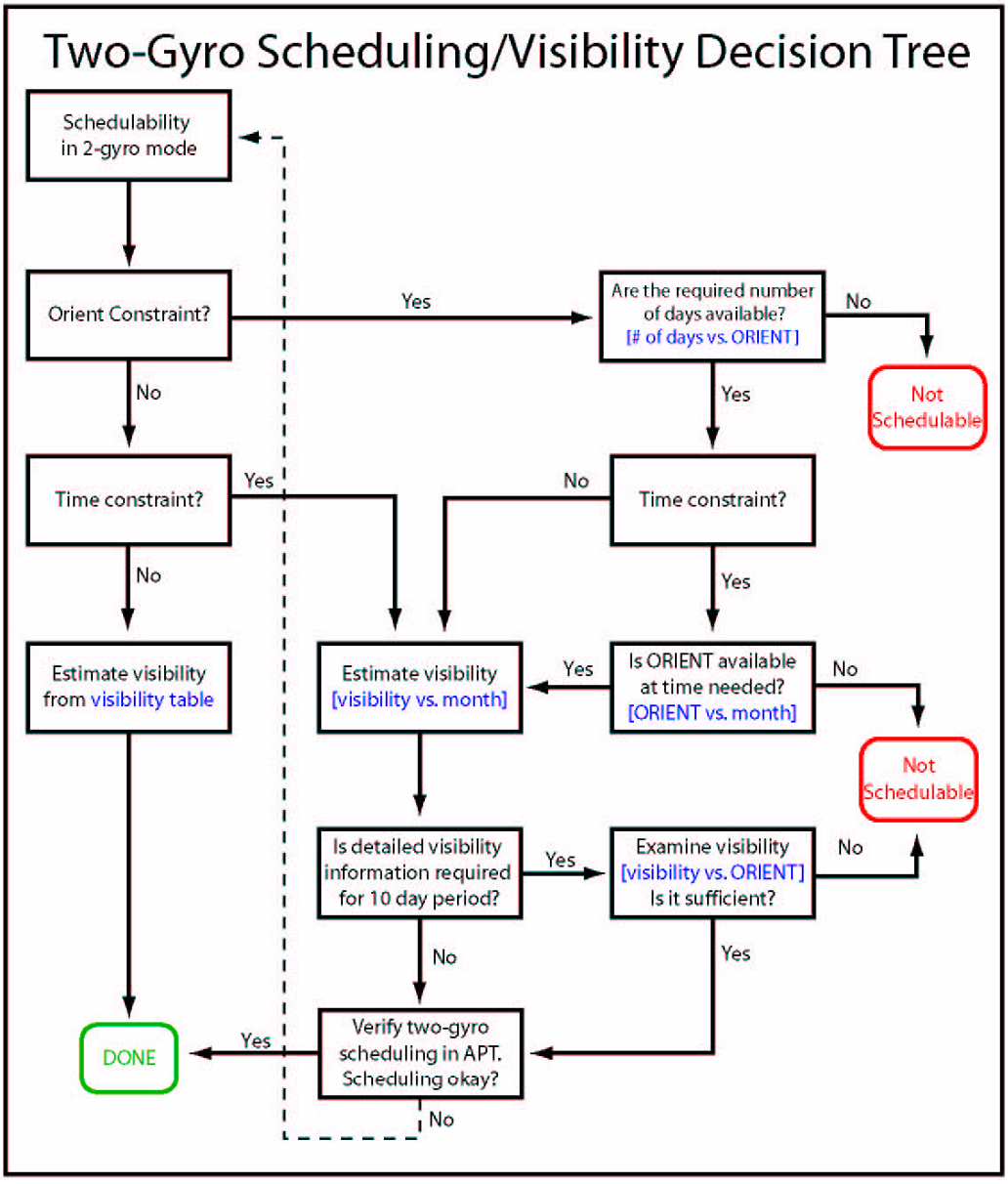

2.3.2 Unconstrained Fixed-Target Observations

If you do not need to specify the orientation of the observatory or the time of year of the observation, then the impact on scheduling is minimized and the observation will be schedulable at some time during the year. The orbital visibility of an unconstrained fixed-target is determined primarily

by its declination. Table 2.1 lists the two-gyro orbital visibility periods as a function of declination. These average values are sufficient for Phase I orbit calculations.

Table 2.1: Standard Two-Gyro Fixed-Target Orbital Visibility Periods

Declination (degrees)	Orbital Visibility[1] (minutes)	LOW Visibility[2] (minutes)	SHADOW Visibility[3] (minutes)
0–5	52	47	25
5–15	52	47	25
15–25	53	48	25
25–35	53	48	25
35–45	53	48	25
45–55	54	45	25
55–65	54	45	25
65–75	55	43	25
≥75	57	42	25
Any CVZ	96	incompatible	incompatible

1. The orbital visibility periods in this table are the typical unocculted times available for guide star acquisitions and instrument-related activities.
2. LOW visibility refers to low-sky observations specified with the LOW special requirement.
3. SHADOW visibility refers to Earth-shadow observations specified with the SHADOW special requirement.

If your observation has no timing or orientation special requirements, the orbital visibility period can be found in Table 2.1, and you do not need to use the scheduling plots found later in this chapter or on the Two-Gyro Science Mode web site.

2.3.3 Constrained Fixed-Target Observations

If your science goals require specification of either the orientation of the observatory and/or the timing of the observation, determinations of the schedulability and orbital visibility period are slightly more complicated.

An on-line tool to help you determine when a fixed target can be scheduled during Cycle 15 is available on the Two-Gyro Science web page at:

http://www.stsci.edu/hst/HST_overview/TwoGyroMode/AllSkyInformation

Enter the coordinates of your target into the web form, and the tool provides several graphical products that can be used to assess when and for how long the target is visible. The calculations used to construct this output were performed on a 5˚x5˚ grid on the sky. The output returned is appropriate for the grid point nearest the input coordinates. Thus, any input position is within 3.5 degrees of a grid point. This sampling is sufficient to provide accurate scheduling and visibility information for any position on the sky for the Phase I proposal process. The models used as input to produce this information rely upon realistic representations of the constraints expected for two-gyro operations. For clarity, Moon avoidance constraints are not included in these results; this does not alter the schedulability of a fixed-target or its orbital visibility significantly. Complete models including all constraints will be available for Phase II proposal processing.

The products returned by the Available Science Time and Orientation web tool include:

1. A plot and table of the total number of days per year that each orientation is available.
2. A plot and table of when each orientation is available during Cycle 15 and the first half of Cycle 16.
3. A plot and table of the target visibility as a function of date during Cycle 15 and the first half of Cycle 16.

The plots contain information about the schedulability of the target and how much time per orbit is available for the observation. Examples of each of these plots and tables are discussed below.

Plot Example: Number of Available Days as a Function of Orientation

The number of days that a particular HST orientation (roll angle) can be achieved in two-gyro mode in Cycle 15 is shown as a function of orientation for a low-latitude location ($\alpha = 0^\circ$, $\delta = 0^\circ$) in Figure 2.4 and for a high-latitude location ($\alpha = 0^\circ$, $\delta = +70^\circ$) in Figure 2.5. An available day is defined to be one in which at least one orbit with the nominal visibility listed in Table 2.1 exists (red curve in the figures). Some days may have only short visibility periods; for reference, the number of days with visibilities ≥30 minutes is also plotted in the figures (blue curve). A portion of the table returned by the web tool for the low latitude example is provided in Table 2.2.

The number of days of availability may be quite limited for some orientations, especially at low declinations, as a result of Sun angle constraints. The range of available orientations expands at higher latitudes,

with the number of days of availability increasing for some orientations and decreasing for others. In some cases, the number of days available may be zero.

In the low latitude example in Figure 2.4, there is a restricted range of orientations over which the target is observable. There is minimal availability for orientations from 0˚-30˚ and from 280˚-360˚. There is a large window available for orientations centered around 245˚, and using orbits with less than the nominal (52 minute) visibility does not increase the availability significantly. Note that, unlike three-gyro operations, it is not possible to observe at orientations with a 180˚ separation.

Figure 2.4: Orientation Availability for a Low-Latitude Target Near $\alpha = 0^{\circ}$, $\delta = 0^{\circ}$

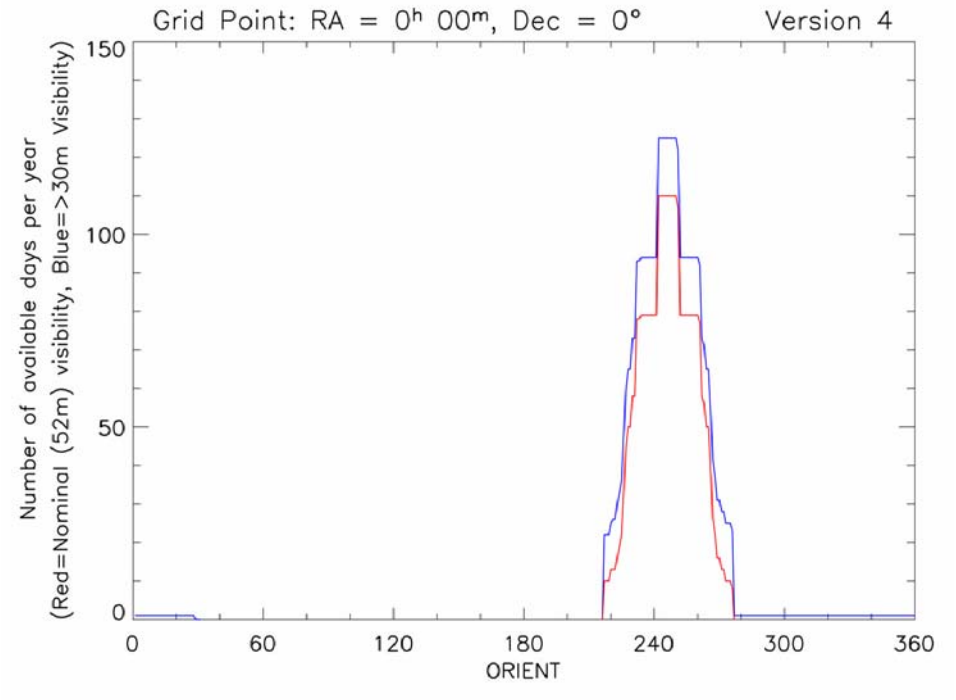

In the high latitude example in Figure 2.5, many orientations are available for five or more days, with notable exceptions occurring over restricted ranges in orientation where the availability dips to zero. Unlike the low latitude case, there are several orientations (e.g., 180˚) for which the use of orbits with less than nominal (55 minute) visibility increases the availability; in some cases, the target is available only with these short orbits. However, scheduling these short orbits results in efficient use of the telescope. Requests for short orbits must be well-justified scientifically and are expected to be available only in exceptional cases.

Table 2.2: A Portion of the Tabular Output for the Data Shown in Figure 2.4

Grid Point: RA = 0^h 00^m, Dec = 0°		
Orientation Angle (deg)	**Number of Days Available (>30 min)**	**Number of Days Available (>52 min)**
:	:	:
262	73	58
263	71	56
264	65	50
265	65	50
266	54	39
267	41	26
268	37	22
269	31	16
270	31	16
271	28	13
272	28	13
:	:	:

Figure 2.5: Orientation Availability for a High-Latitude Target at $\alpha = 0^\circ$, $\delta = +70^\circ$

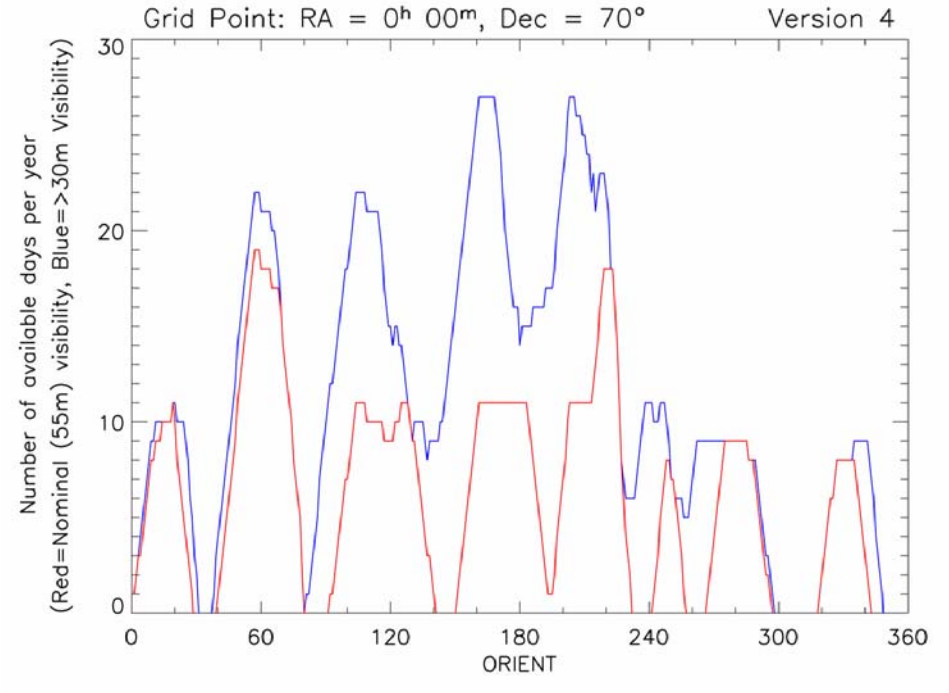

Plot Example: Availability of Roll Angles in Cycle 15

If a sufficient number of days exists to observe a target, the next step in determining its schedulability is to check when the target could be scheduled. If there are roll angle (`ORIENT`) constraints, you should check when the particular orientation is available by examining the web tool plot illustrating `ORIENT` versus time. Example plots are shown in Figure 2.6 and Figure 2.7, and a sample of the tabular output is shown in Table 2.3. The time axis on these plots extends for 18 months from the start of Cycle 15 (1 July 2006 to 31-Dec-2007) so that observers can judge whether observations that may begin in Cycle 15 could be concluded in the first half of Cycle 16. The blue regions of the figures indicate what orientations are available for the specified date when there is at least one orbit with 30 minutes of visibility. The gold regions indicate less than 30 minutes of visibility for some ORIENTs on that date. Note that most orientations are available only for limited periods of time.

Consider first the low-latitude pointing in Figure 2.6. The February-May time period is unavailable because of Sun avoidance restrictions. The Sun-leading region of the sky (October-February) is also inaccessible in two-gyro mode because of the need for fixed-head star tracker (FHST) visibility prior to fine-lock. Thus, in 2006, available orientations are limited to the June-September timeframe. A somewhat larger range of orientations is accessible for a very restricted range of dates in late September 2006 and 2007 when the target is located near the anti-Sun direction.

Figure 2.6: Low-Latitude Target Roll Angles Available During Cycle 15

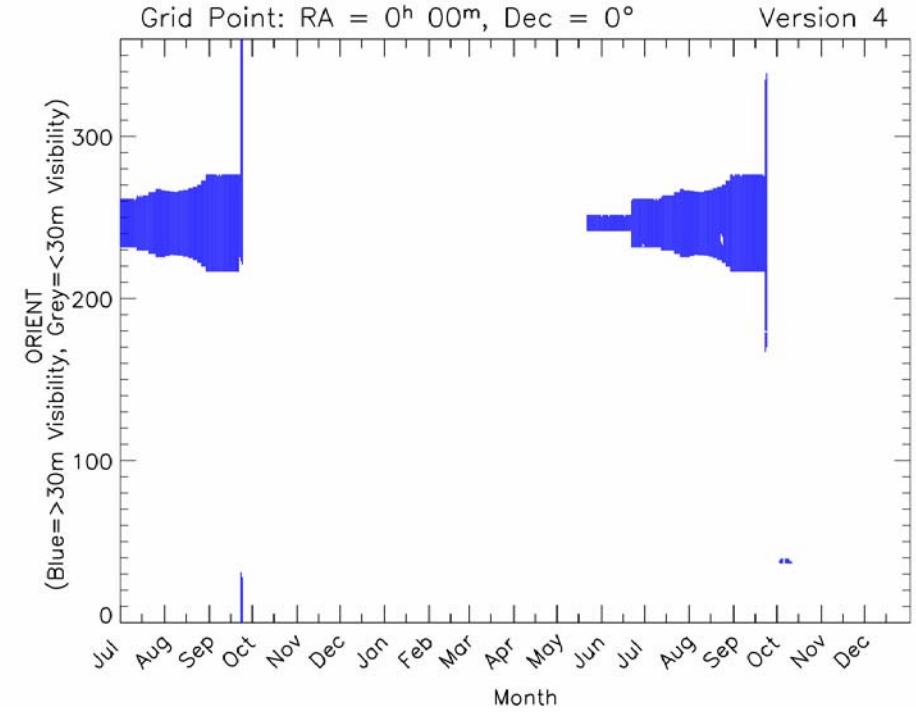

For the high latitude pointing in Figure 2.7, the availability of roll angles in two-gyro mode is broken into several time intervals separated by periods where the object is unobservable. These breaks in availability occur primarily because precession of the HST orbit causes the Earth to block the FHSTs, which are needed for guide star acquisitions.

Table 2.3: A Portion of the Tabular Output for the Data Shown in Figure 2.6

Grid Point: RA = 0^h 00^m, Dec = 0°	
Date	**Available Orientations**
:	:
20-Sep-2006	216.6 - 276.6
21-Sep-2006	216.6 - 276.
22-Sep-2006	225.6 - 276.6
23-Sep-2006	223.0 - 31.0
24-Sep-2006	221.0 - 28.0
22-May-2007	241.6 - 251.6
23-May-2007	241.6 - 251.6
24-May-2007	241.6 - 251.6
25-May-2007	241.6 - 251.6
:	:

Figure 2.7: High-Latitude Target Roll Angles Available in Cycle 15

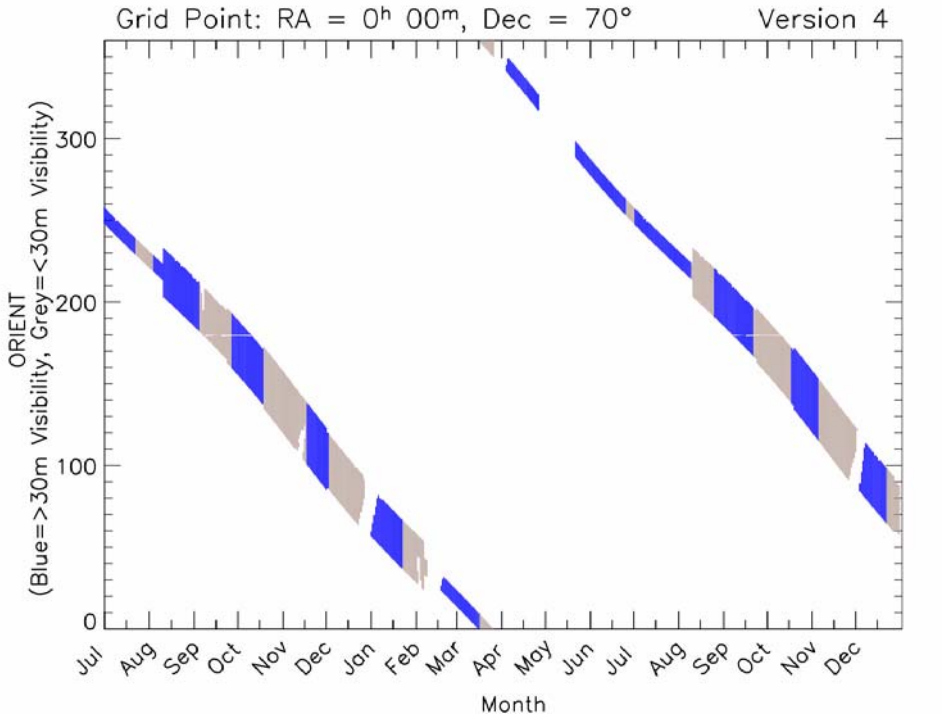

Plot Example: Target Visibility as a Function of Date

For constrained observations, the orbit visibility may change dramatically throughout the year, unlike unconstrained observations, the visibility cannot be described as a simple function of declination alone (e.g., Table 2.1). The web tool displays the visibility information in graphical form in a plot of target visibility versus time for an 18 month period beginning at the start of Cycle 15 (1 July 2006 to 31-Dec-2007). Plots for the low- and high-latitude sight lines are shown in Figure 2.8 and Figure 2.9. Sample tabular output for Figure 2.8 is shown in Table 2.4. The orbital visibilities in these plots are shown with blue points indicating the maximum visibility available, and by green lines indicating the full range of visibilities for the orientations available. In some instances, the maximum visibility depicted by the blue line may be identical to the minimum visibility in which case there is no green line, just a blue point.

The horizontal black line at 30 minutes in Figure 2.8 and Figure 2.9 indicates the minimum orbital visibility that will be allowed for Phase I proposals in Cycle 15 without special scientific justification. Most observations can be scheduled at times when the orbital visibility exceeds this amount, and those few that cannot will likely have other restrictions that will preclude such observations. For example, in the high-latitude example, the visibility window on 11 September 2006 is only 10 minutes. Therefore, a target at this location in the sky will not be scheduled on this date.

Figure 2.8: Orbital Visibility for a Low-Latitude Target in Cycle 15

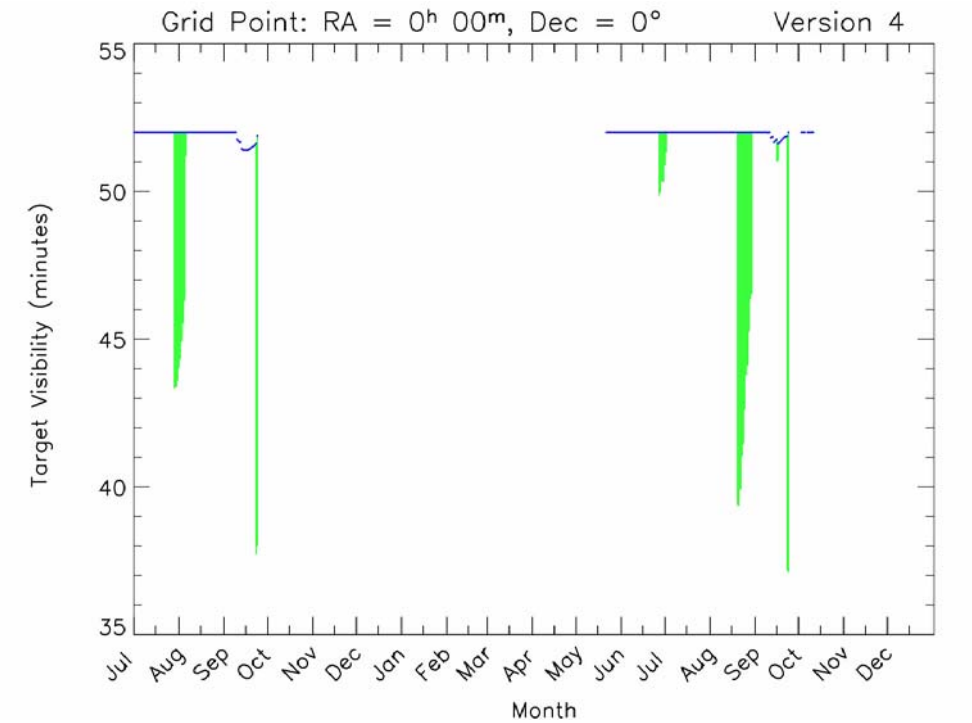

Table 2.4: A Portion of the Tabular Output for the Data Shown in Figure 2.8

Grid Point: RA = 0^h 00^m, Dec = 0°		
Date	**Science Time Available (minutes)**	
	Two-Gyro (minimum)	**Two-Gyro (maximum)**
:	:	:
26-Jul-2006	52.0	52.0
27-Jul-2006	52.0	52.0
28-Jul-2006	52.0	52.0
29-Jul-2006	43.3	52.0
30-Jul-2006	43.4	52.0
31-Jul-2006	43.6	52.0
01-Aug-2006	44.0	52.0
02-Aug-2006	44.3	52.0
03-Aug-2006	44.9	52.0
04-Aug-2006	45.5	52.0
:	:	:

Figure 2.9: Orbital Visibility for a High-Latitude Target in Cycle 15

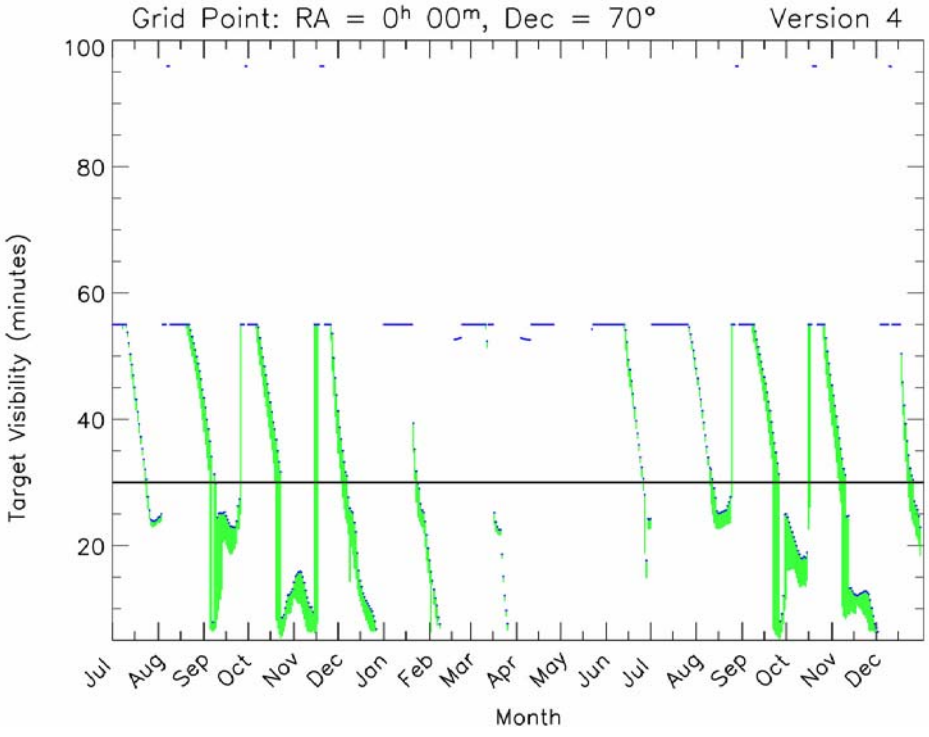

In calculating the orbit visibility period in two-gyro mode for Cycle 15, observers should adopt the maximum visibility estimate indicated by the blue points in the visibility plots unless they have both `ORIENT` and timing restrictions, in which case they need to examine the more detailed visibility plots described in the next section. The HST scheduling system will make every effort to schedule observations when the visibility is optimized.

Detailed Target Visibility Considerations

In some cases it may be necessary to have a more detailed look at the target visibility for various orientations on a particular date to assess whether a highly constrained observation is feasible. The Detailed Visibility Tool on the Two-Gyro Science Mode web page can be used to determine the target visibility. You can enter the target coordinates and the desired date of the observation, and the tool will return a plot and table of the science time available as a function of orientation for the 11 day interval centered on the input date.

Figure 2.10 contains an example of the detailed visibility plot for the low-latitude sight line example on a set of dates centered on 20 August 2007. The resulting visibilities are color coded by date. The information is shown in tabular form in Table 2.5. Observers requiring a specific orientation on a specific date should specify the appropriate visibility indicated by these plots (or tables) in their Phase I proposals.

Figure 2.10: Detailed Visibility Plot for a Low-Latitude Target

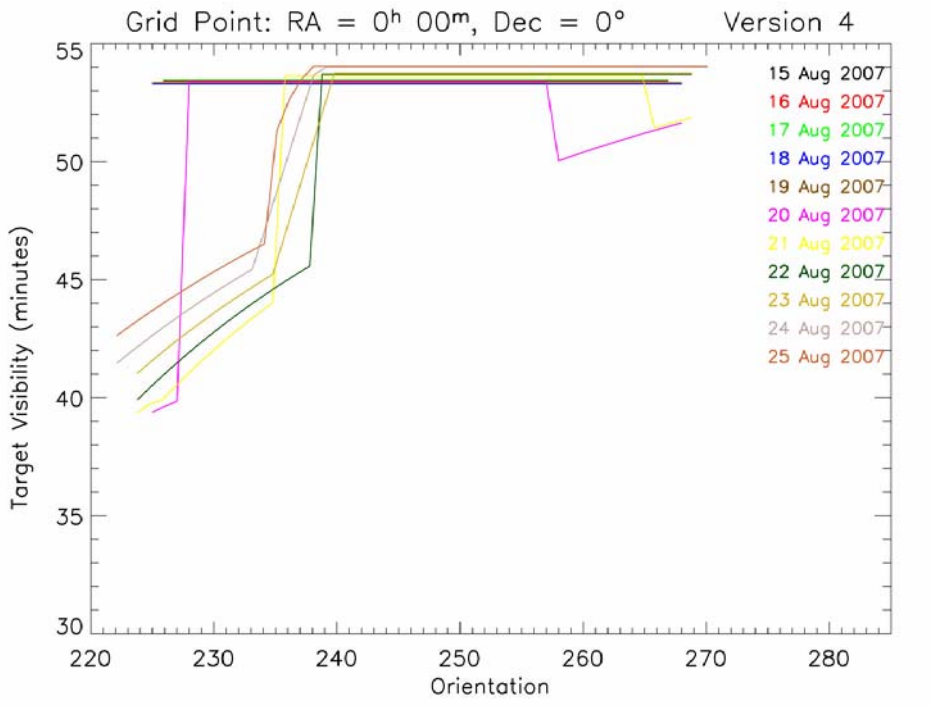

Table 2.5: A portion of the Tabular Output for the Data Shown in Figure 2.10

Orient	Year 2007	Orbital Visibility (minutes)									
	Aug 15	Aug 16	Aug 17	Aug 18	Aug 19	Aug 20	Aug 21	Aug 22	Aug 23	Aug 24	Aug 25
222	0	0	0	0	0	0	0	0	0	41	43
223	0	0	0	0	0	0	0	0	0	42	43
224	0	0	0	0	0	0	39	40	41	42	43
225	0	0	0	53	53	39	40	40	41	43	44
226	53	53	53	53	53	40	40	41	42	43	44
227	53	53	53	53	53	40	40	41	42	43	44
235	53	53	53	53	53	53	44	45	45	0	51
:	:	:	:	:	:	:	:	:	:	:	:
266	53	53	53	53	53	51	51	54	54	54	54
267	53	53	53	53	53	52	52	54	54	54	54
268	0	0	0	53	53	52	52	54	54	54	54
269	0	0	0	0	0	0	52	54	54	54	54
270	0	0	0	0	0	0	0	0	0	54	54

2.3.4 Examples

In this section we provide some examples of how to determine the schedulability and visibility period for different types of observations in two-gyro mode.

`Example 1: Time-series observations of the Hubble Deep Field (HDF) and Hubble Ultra Deep Field (HUDF).`

Observer #1 wants to search for supernovae in the HDF and HUDF by repeating a set of ACS observations every ~45 days for as many consecutive 45-day intervals as possible. The fields are tiled with multiple pointings, each of which has five 400 second integrations designed to fit in a single orbit. The total time required to tile either field is 15 orbits (~1 day). Orientation is not critical, as the field can be tiled in a manner that allows nearly full coverage of the field regardless of orientation. The HDF and HUDF are located at $\alpha = 12^h\ 32^m$, $\delta = +62^\circ 18'$ and $\alpha = 3^h\ 32^m$, $\delta = -27^\circ\ 55'$, respectively.

Figure 2.11: Time Available per Orbit for the HDF in Cycle 15

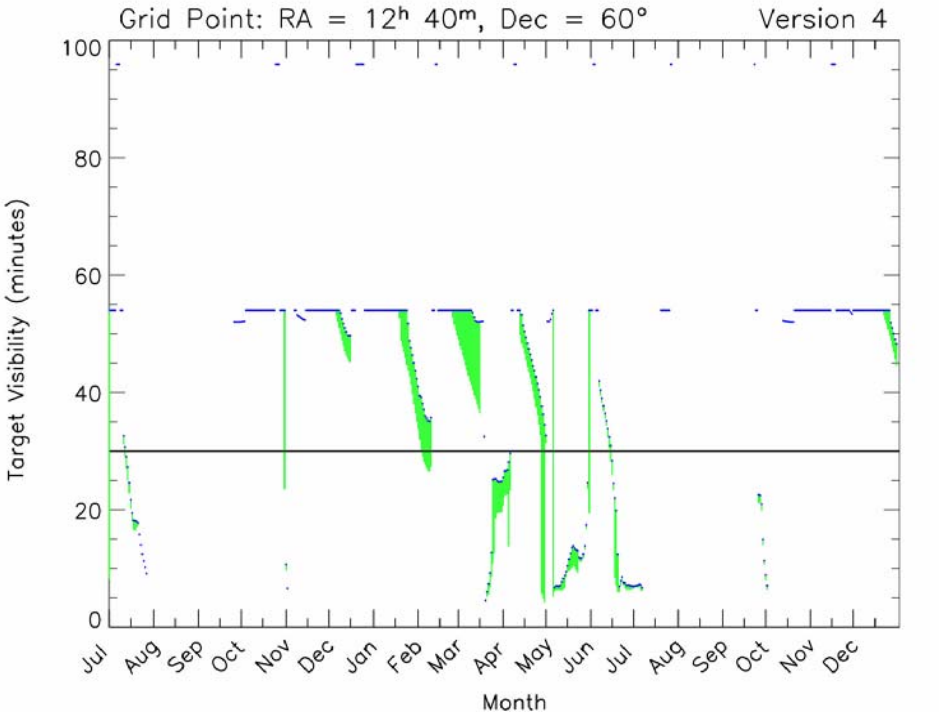

Let's consider first the HDF. Using the on-line tool available at the Two-Gyro Science web site, we examine the scheduling and visibility plots available for the $\alpha = 12^h\ 40^m$, $\delta = 60^\circ$ grid point. The plot of number of available days versus orientation shows that there are many days in Cycle 15 that the HDF is observable in two-gyro mode provided that the orientation is greater than ~130 degrees. Since Observer #1 does not have an orientation constraint, we skip the plot of orientation versus month and proceed directly to the plot of visibility versus month. From this plot (Figure 2.11), we see that good visibility is achievable for this program throughout much of the year.

This program could be conducted with a set of 4 observing opportunities spaced ~45 days apart (e.g., 01-Oct-2006, 14-Nov-2006, 29-Dec-2006, 12-Feb-2007). The science times available per orbit on these dates are listed in Table 2.6. A larger set of observations may be difficult to schedule since the next opportunity in this set (March 29) has very poor visibility. When dealing with visibilities that change rapidly over the course of a month, flexibility in time series spacing may improve the schedulability. For example, in this case allowing a 55 day separation from February 12 to April 8, instead of the 45 day spacing between February 12 and March 29, would increase the visibility sufficiently to make another epoch of observations possible.

Table 2.6: Two-Gyro Time for the HDF on Selected Dates in Cycle 15

Observation Date	Time per Orbit (minutes)
01-Oct-2006	52
13-Nov-2006	53
14-Nov-2006	52
15-Nov-2006	54
28-Dec-2006	54
29-Dec-2006	54
30-Dec-2006	54
11-Feb-2007	54
12-Feb-2007	54
13-Feb-2007	96
28-Mar-2007	25
29-Mar-2007	25
30-Mar-2007	25

Now consider the HUDF. Using the on-line tool available at the Two-Gyro Science web site, we examine the scheduling and visibility plots available for the $\alpha = 3^h\ 40^m$, $\delta = -30^\circ$ grid point. The possibilities for scheduling a series of observations with a spacing of 45 days is more limited due to the gap from mid-December 2006 to June 2007. Starting the series as early as possible is the only way to obtain four observing opportunities.

Table 2.7: Two-Gyro Time for the HUDF on Selected Dates in Cycle 15

Observation Date	Time per Orbit (minutes)
01-Jul-2006	53
14-Aug-2006	53
28-Sep-2006	57
12-Nov-2006	52

Figure 2.12: Time Available per Orbit for the HUDF in Cycle 15

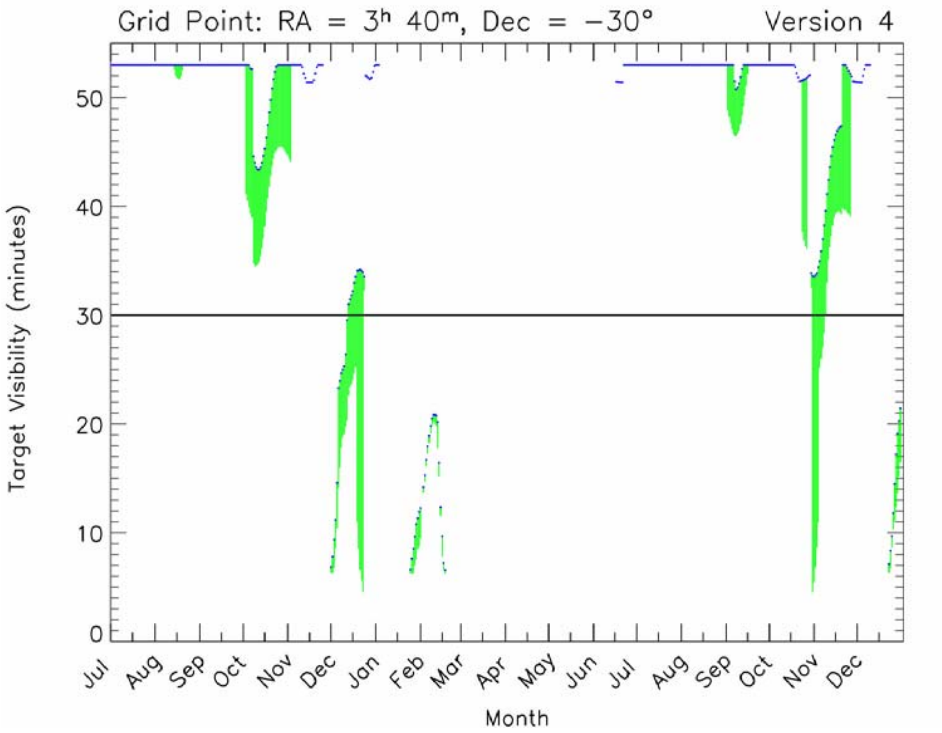

Example 2: Time-series light curve observations of a supernova found in Example 1.

Observer #1 finds a supernova in the HDF using the experiment outlined in Example 1 and wants to obtain the light curve of the supernova by obtaining photometric images of the supernova and surrounding field once a week for 7 weeks. The supernova was discovered after the fourth set of observations was obtained on 12 February 2007.

Using the visibility versus month plot generated for Example 1, Observer #1 notes that the orbital visibilities for the HDF and surrounding areas are good on February 19 and 26 (54 minutes) as well as March 5 and 12 (54 and 53 min, respectively). However, by March 19 the visibility has dropped to 33 minutes, and by March 26 it is only 25 minutes. Thus, it is not possible to follow the supernova light curve throughout the entire 45 day period as hoped.

If the supernova had been found after the second epoch observations of the HUDF (instead of the HDF), it would have been possible to follow the light curve for the full 45 day interval between 14 August 2006 and 2 October 2006 (see Figure 2.12).

Example 3: Time-constrained observations of recurrent nova T Pyx.

Observer #3 wants to observe the recurrent nova T Pyx ($\alpha = 9^h\ 05^m$, δ = -32˚ 23') during its next outburst, which should begin in early October 2006. The objective is to study the evolution of the ejected shell using images (3 orbits with at least 46 minutes of visibility) obtained as soon as possible after outburst, followed by images 7, 21, 49, 84, 112, 140, and 365 days later. There are no orientation constraints on the observations. Observer #3 estimates the science time available using the web tool plot of visibility versus month shown in Figure 2.13 for the nearby position at $\alpha = 9^h\ 0^m$, δ = -30˚ (see also Table 2.8).

Figure 2.13: Time Available for T Pyx in Cycle 15

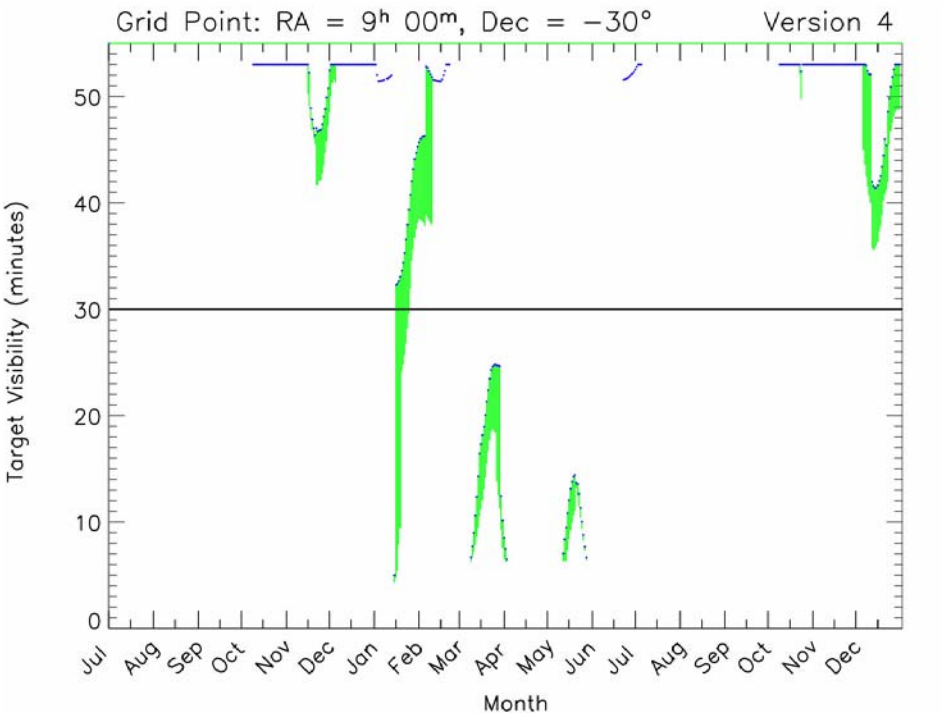

Examination of this plot provides the following information (assuming a 9 October 2006 start) for the relative timing of the observations and the amount of science time available per orbit.

Table 2.8: Two-Gyro Time Available for T Pyx on Selected Cycle 15 Dates

Observation Date	Relative Timing (days)	Time per Orbit (minutes)
09-Oct-2006	0	53
16-Oct-2006	7	53
30-Oct-2006	21	53
27-Nov-2006	49	48
01-Jan-2007	84	53
29-Jan-2007	112	44
26-Feb-2007	140	0
09-Oct-2007	365	53

Two of the observations have less than the 46 minutes of visibility needed for this particular science investigation, and are therefore not suitable choices for this time series. The day 112 observation would need to be moved back to February 3, while the day 140 observation would need to be moved to February 22. Since these observations have moved closer together, Observer #3 decides to drop the day 140 observation. A possible revised series of observations is given in Table 2.9.

Table 2.9: Revised Two-Gyro Time Series for T Pyx in Cycle 15

Observation Date	Relative Timing (days)	Time per Orbit (minutes)
09-Oct-2006	0	53
16-Oct-2006	7	53
30-Oct-2006	21	53
27-Nov-2006	49	48
03-Feb-2007	117	46
09-Oct-2007	365	51

However, while the outburst is expected around the beginning of October, it could occur later in the month, so it is necessary to check how a later outburst would impact the observations. With start dates of October 16, 23, and 30, the following sequences listed in Table 2.10 are possible. Thus, if T Pyx goes into outburst anytime in October, the observations can be successfully obtained in two-gyro mode.

Table 2.10: Alternate Time Series for T Pyx in Cycle 15

Observation Date/Timing	Time per Orbit (minutes)	Observation Date/Timing	Time per Orbit (minutes)	Observation Date/Timing	Time per Orbit (minutes)
16-Oct-2006 / 0	53	23-Oct-2006 / 0	53	30-Oct-2006 / 0	53
23-Oct-2006 / 7	53	30-Oct-2006 / 7	53	06-Nov-2006 / 7	53
06-Nov-2006 / 21	53	13-Nov-2006 / 21	53	20-Nov-2006 / 21	47
04-Dec-2006 / 49	53	11-Dec-2006 / 49	53	18-Dec-2006 / 49	53
08-Jan-2007 / 84	52	...	...	...	...
05-Feb-2007 / 112	46	12-Feb-2007 / 112	52	19-Feb-2007 / 112	52
16-Oct-2007 / 365	53	23-Oct-2007 / 365	53	30-Oct-2007 / 365	53

Example 4: An orientation-constrained observation of the Vela supernova remnant.

Observer #4 wants to take an ACS image of a portion of the Vela supernova remnant near the position of the star HD 72089 ($\alpha = 08^h\ 29^m$, $\delta = -45^\circ\ 33'$). A roll angle of 70±5 degrees must be used to keep the bright star off the detector. A second observation to observe a different part of the remnant requires an orientation 90±5 degrees from the first observation.

Entering the coordinates of HD 72089 into the scheduling tool on the web yields the following plots of the number of days each orientation is available (Figure 2.14) and orientation versus month (Figure 2.15) for the nearby position at $\alpha = 8^h\ 20^m$, $\delta = -45^\circ$. It is apparent from these plots that an orientation of 70 degrees cannot be achieved in two-gyro mode at any time in Cycle 15.

Realizing that the planned orientations are not viable, Observer #4 checks the availability of orientations 180 degrees from those originally envisioned. The inverse orientations at 250 degrees and 340 degrees are accessible in October 2006 and December 2006, respectively. Therefore, this observation is feasible in two-gyro mode as long as the requested orientations are changed to 250±5 degrees and 340±5 degrees. The availability of allowable orientations must be described appropriately in the Phase I proposal.

Figure 2.14: Cycle 15 Orientation Availability in the Direction of the Vela SNR

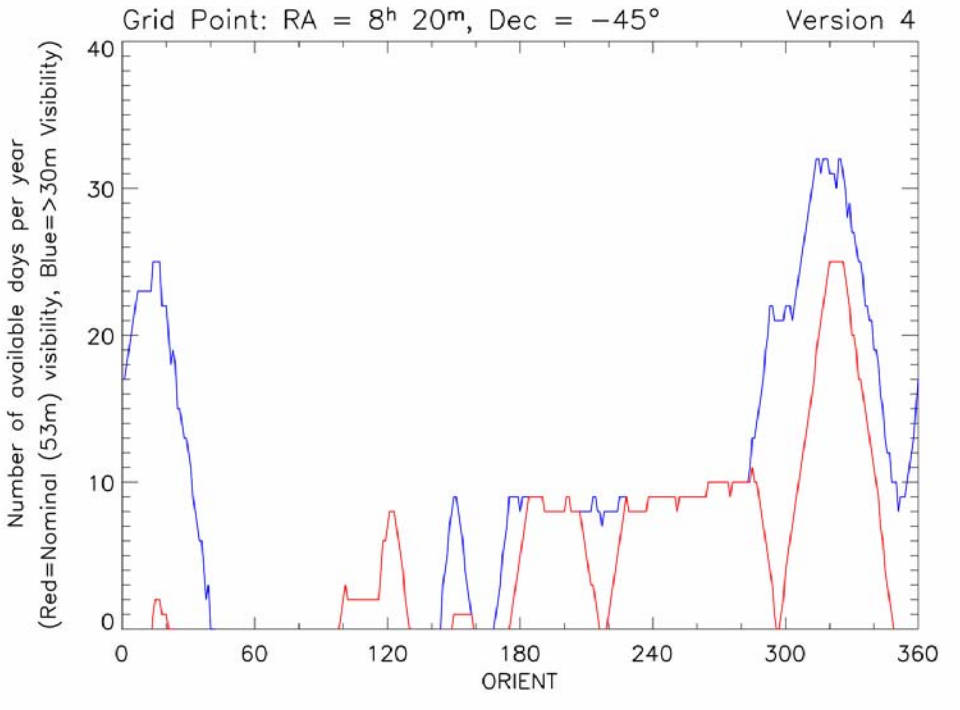

Figure 2.15: Cycle 15 Orientation Angles Versus Month Toward the Vela SNR

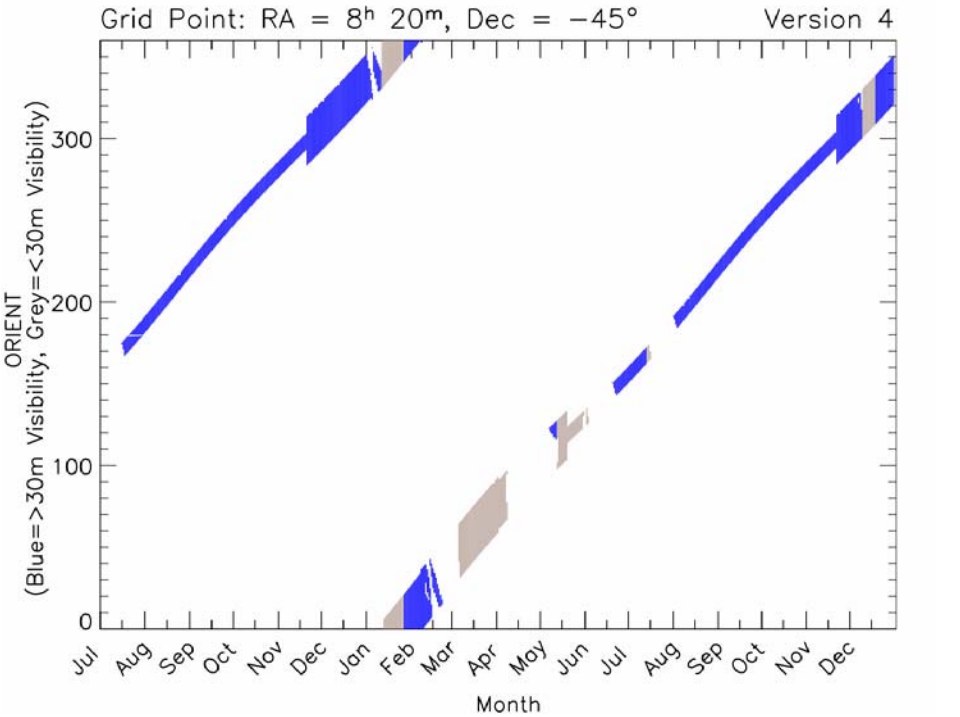

2.4 Verifying Scheduling Constraints for Phase I

The Astronomer's Proposal Tool (APT) package contains software to check the schedulability of targets in Phase I proposal forms. When filling out the APT form for their Phase I proposals, Cycle 15 proposers will be asked to verify the availability of their targets in two-gyro mode. Observers should perform this check after they have entered their observation information based upon the tables and plots discussed in the previous sections of this chapter.

2.5 Two-Gyro Orbit Calculations for Phase I

The visibility period for two-gyro observations should make use of the two-gyro visibility periods from the plots and tables described in this chapter. The tools for creating these plots and tables are available on the Two-Gyro Science Mode web site. Exposure times for two-gyro observations should be calculated with the appropriate two-gyro exposure time calculators (ETCs) for each instrument. In most cases, these are the same ETCs as were used for three-gyro mode since the instrument performance in both cases is nearly indistinguishable. Links to these ETCs can be found on the main web page for each instrument.

2.6 Continuous Viewing Zones

The continuous viewing zones (CVZs) are regions of the sky where HST can observe without interruptions caused by target occultation by the Earth. These zones are approximately 24 degrees in size centered on the orbital poles, which are 28.5 degrees from the celestial poles. Thus, targets located in declination bands near ±61.5 degrees may be in the CVZ at some time during the 56-day HST orbital precession cycle. The CVZ interval duration depends upon the telescope orbit, target position, and constraints imposed by Sun and Earth limb avoidance. South Atlantic Anomaly crossings limit the uninterrupted visibility of any target to no more than 5-6 orbits (see Section 2.3.2 in the *HST Primer*).

The CVZs in two-gyro mode will be the same size as those in three-gyro mode, but the durations may be shorter because of more restrictive pointing constraints. To determine whether constrained two-gyro observations qualify for CVZ time, observers should consult the visibility tables and plots, like those discussed above. Only those observations for which the orbital visibility is 96 minutes should be considered CVZ candidates.

2.7 Moving Targets

We expect that there will be no significant impact of two-gyro operations on moving target observations other than that gyro-only tracking and guide star handoffs are not available in two-gyro mode. Proposers wanting to observe moving targets should consult the Two-Gyro Science Mode web page for updates, which will be posted as information about observing moving targets in two-gyro mode becomes available.

CHAPTER 3:

The HST Gyroscopes

In this Chapter...

3.1 Gyroscope Overview[1]

HST has six rate-sensing gyroscopes. Two of the six gyroscopes are no longer functioning. Under normal operating procedures, three of the six gyros must be functioning to provide sufficiently accurate pointing to achieve guide star acquisitions and science data collection. The gyroscopes aboard HST sense whenever the attitude of the observatory is changing, whether during large angle slews from one target to another or during small pointing changes as a result of subtle forces acting upon the observatory. Each gyroscope senses the motion about a single axis. The relative orientations of the gyro axes within HST are different so that the torques exerted on the gyroscopes by attitude changes affect each gyro differently. As a result, any combination of three gyros can be used to define a set of three orthogonal axes around which changes in the roll, pitch, and yaw of the observatory may be measured.

There are many different types of gyroscopes available, but only gas bearing gyros are capable of providing the combination of extremely low noise, excellent stability, and high sensitivity to motions that is required for HST observations. Each gyro has a wheel spinning at a constant rate of 19,200 rotations per minute on gas bearings. The wheel is mounted in a sealed cylinder, which floats in a thick fluid. Electricity is carried to the motor that spins this wheel by thin wires, or flex leads, approximately the

1. Some of the information in this chapter was reproduced from the *Hubble Space Telescope Gyroscopes Hubble Facts sheet* available from the GSFC HST Program Office.

width of a human hair. The wires are immersed in the fluid along with the wheel. Changes in the gyroscope rates induced by movement of HST are captured by onboard electronics. This information is then fed to Hubble's central computer where it is analyzed. The HST pointing is changed through the use of several reaction wheel assemblies. Each assembly contains spinning wheels, which when spun at varying rates, create the appropriate torques required for the desired movement.

The gyroscopes are packaged in pairs, in devices called rate sensing units (RSUs). Each RSU weighs approximately 24.3 pounds and is 12.8 x 10.5 x 8.9 inches in size. The individual gyroscopes weigh approximately 6 pounds and are 2.75 x 6.5 inches in size. Figure 3.1 shows an exploded view of one of the HST gyroscopes. Figure 3.2 shows a gyro after assembly.

Figure 3.1: Exploded View of a Gas Bearing Gyroscope

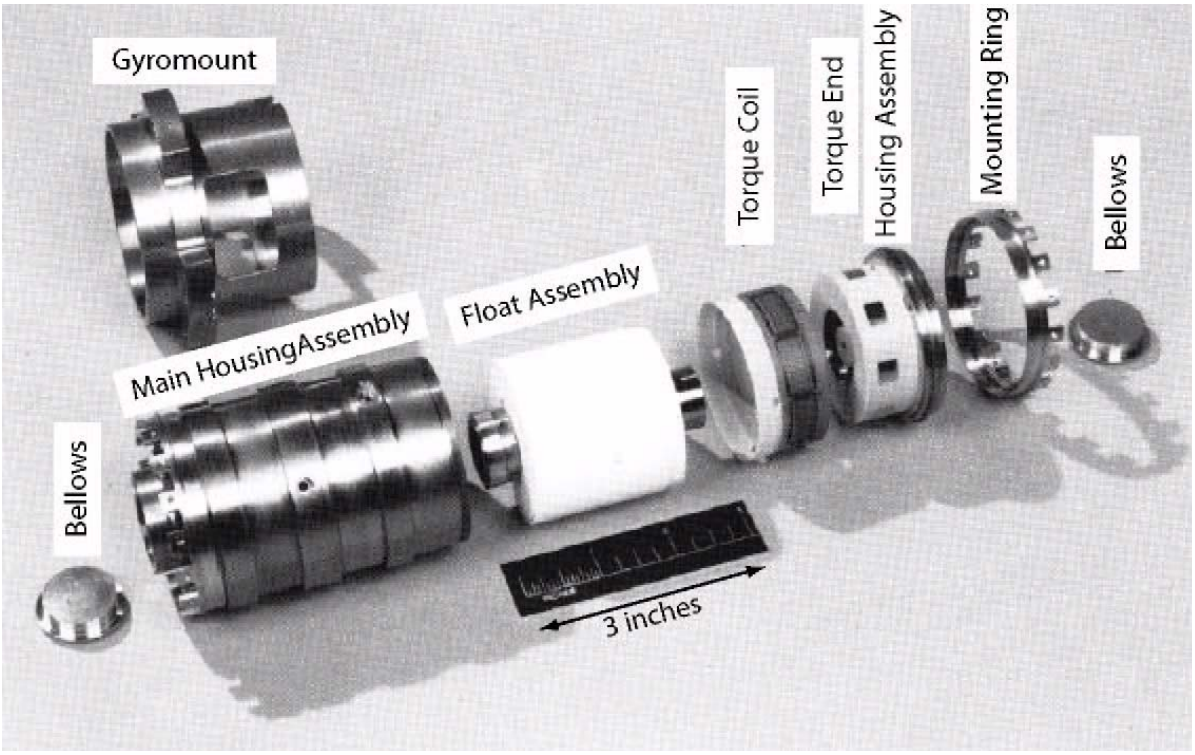

Figure 3.2: Assembled Gyroscope

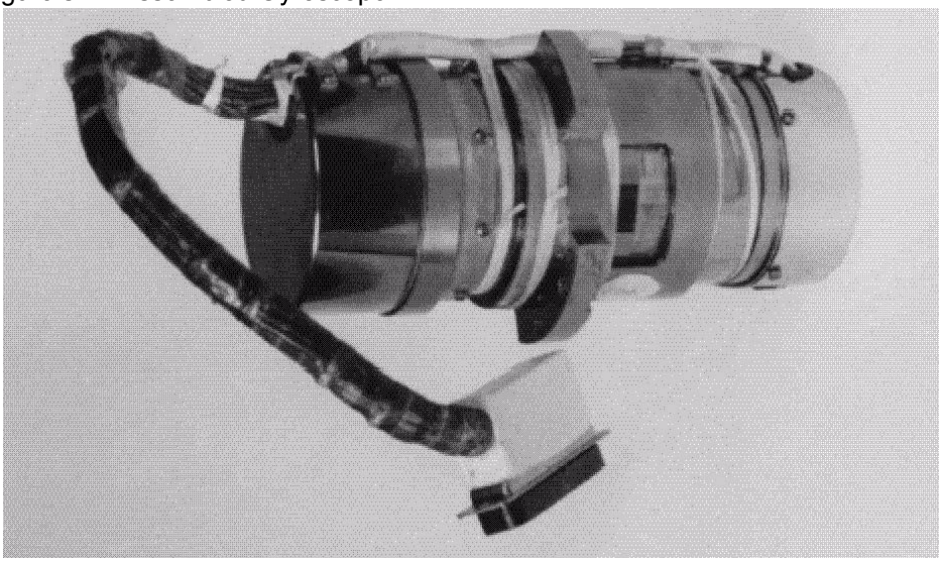

Figure 3.3: Schematic of the Hubble Space Telescope after Servicing Mission 3B

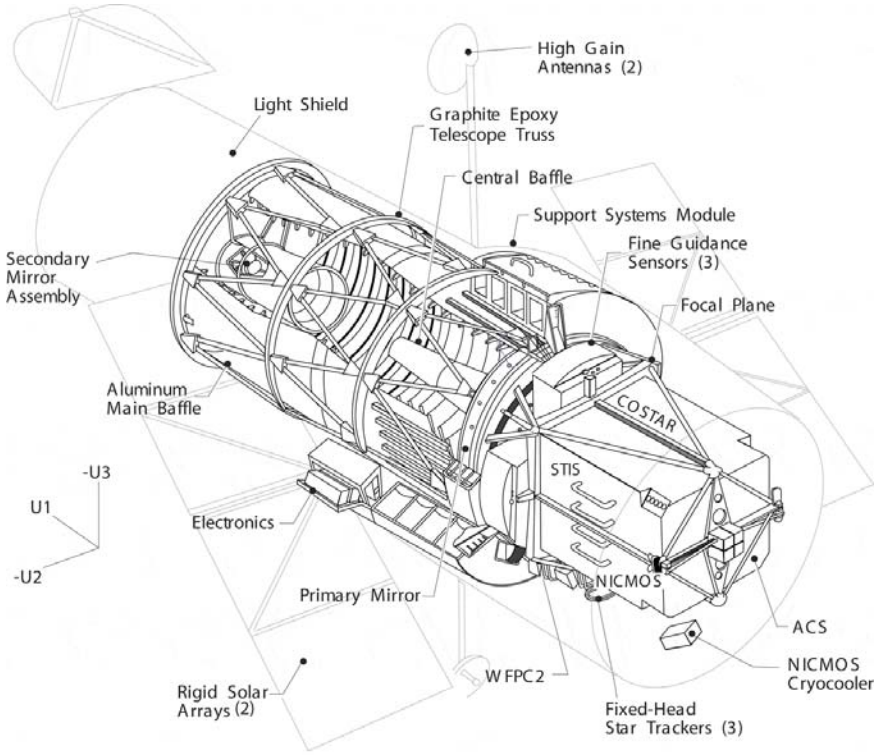

Major components are labelled, and definitions of the **U1**, **-U2**, **-U3 (V1**, **V2**, **V3)** spacecraft axes are indicated.

The HST gyroscopes are attached to the focal plane structure at the aft end of the observatory on the same side as the fixed-head star trackers (FHSTs). Figure 3.3 shows the HST field of view following SM3B in the standard HST coordinate system. The RSUs are accessed by opening the large cargo bay doors on the **U3** side of the observatory.

3.2 Previous Gyroscope Replacements

Four of the six original HST gyroscopes were replaced during the first servicing mission (SM1) in December 1993 by astronauts aboard Space Shuttle flight STS-61. In the years after this servicing mission, the HST gyroscopes failed at a higher-than-expected rate. On 13 November 1999, the fourth of six gyroscopes aboard HST failed, leading to a halt of science observations and entry into safe mode. In anticipation of this event, servicing mission 3, which NASA had been planning for several years, was split into two separate missions: SM3A and SM3B. During SM3A (STS-103, December 1999), astronauts replaced all six gyroscopes (three RSUs) with a full complement of improved gyroscopes.

In the time since SM3A, two of the six gyroscopes have failed. The first gyroscope (Gyro #5) failed on 28 April 2001, and the second (Gyro #3) failed on 29 April 2003. Gyros #6 and #4 have been turned off to extend their lifetime; one will be switched back on when one of the two gyroscopes (#1 and #2) currently providing attitude control in two-gyro mode fails.

The gyroscopes aboard HST have failed because of electronics problems, flex lead problems, and rotor restrictions. A manufacturing weakness with a hybrid electrical component prompted the replacement of the gyros on SM1. The flex lead failures that led to the SM3A replacements resulted from corrosion of the thin electrical wires immersed in the fluid inside the gyroscopes. The problem has been addressed in part by using pressurized nitrogen rather than pressurized air containing oxygen during the fluid fill portion of the gyroscope assembly. Some of the gyroscopes that would be installed during SM4 would also have silver plated leads to reduce corrosion. The failures occurring in the current on-orbit gyros appear to be due to some sort of rotor restriction. The restrictions may be caused by patches of lubricant that have built up in the air bearings of the gyros or by small particles that have become lodged between the bearing surfaces. The restrictions prevent the bearings from turning smoothly. The HST Project is currently investigating the use of diamond-like coatings on the bearing surfaces to reduce rotor restrictions. This is the same type of coating used in the NICMOS cryocooler turbine.

CHAPTER 4:

Slewing and Pointing

In this chapter . . .

4.1 Overview

Slewing of HST is much the same in two-gyro mode as in three-gyro mode, with a few important differences. The primary difference between the two modes is the accuracy of the pointing at the ends of slews. In three-gyro mode, the telescope is generally pointed to within 50-100 arcseconds of the target after a 180 degree slew. In two-gyro mode, the pointing error at the end of a slew of any duration can be as large as 10 degrees because the rate change for one axis of control must be supplied by the HST magnetometers rather than by a gyroscope. For this reason, it is necessary to have a different sequence of activities at the ends of slews in two-gyro mode.

The slew rates in two-gyro and three-gyro modes differ slightly. In three-gyro mode, the maximum maneuver rate is ~11 degrees per minute of time with a typical rate of ~6 degrees per minute. In two-gyro mode the maneuver rate is expected to be ~85% of these values. Two-gyro pointing control and constraints are described in the following sections.

4.2 Two-Gyro Coordinate Conventions

To more easily understand the control of the telescope with two gyros, it is convenient to define a reference frame for the gyroscope control directions and the "missing" control axis. Figure 4.1 is an illustration of an orthogonal coordinate system with two gyros (Gyro A and Gyro B). The first axis of the system is defined by the Gyro A measurement axis. The second axis is defined by the cross product of the two measurement axes of Gyro A and Gyro B. This axis is called the G_X axis. The semi-major axis of the jitter ellipse is the direction associated with rotations about the G_x axis. Information for the G_X axis must be supplied by one of the HST pointing control system sensors other than the two functioning gyros, such as the Fine Guidance Sensors. The third axis is defined by the cross product of the second (G_X) and first (G_A) axes. This axis lies in the gyro plane in a direction that is 90° from the G_A axis.

Figure 4.1: Orthogonal Two-Gyro Coordinate System

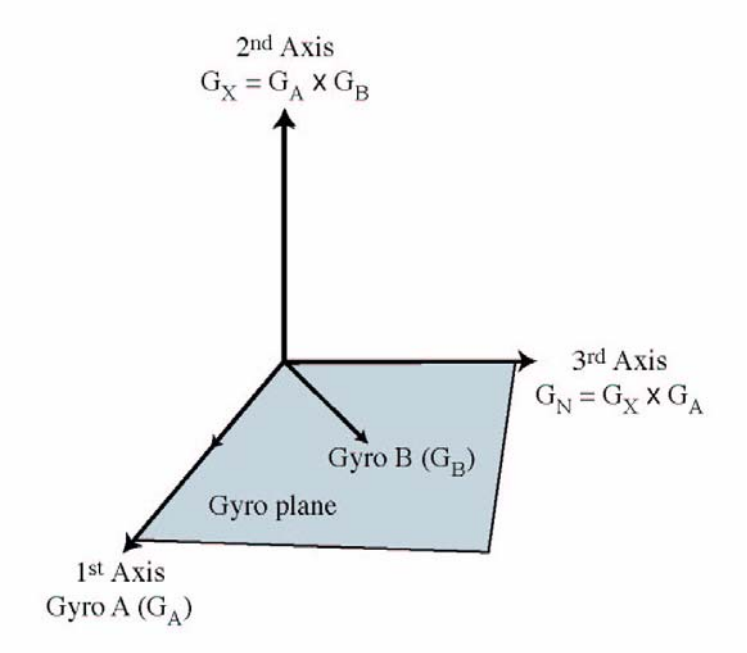

4.3 Pointing Control with Two Gyros

A major rework of the HST attitude control software was necessary to prepare HST for two-gyro operations. This extensive redesign was done by engineers and software experts at the Goddard Space Flight Center. The various control modes described below are part of the updated onboard attitude control system and are invoked automatically when needed.

4.3.1 Magnetic Sensing System and Two Gyros (M2G)

The M2G mode uses two gyros in combination with information about the Earth's magnetic field orientation to provide pointing control. The Magnetic Sensing System (MSS) on HST consists of two magnetometers. The magnetometers measure the strength and direction of the Earth's magnetic field. Together with a model for the magnetic field, they can be used to supply pointing control information for the G_X axis. The typical pointing accuracy in M2G mode is 2-5 degrees but can be as poor as ~10 degrees when the G_X axis is aligned with the Earth's magnetic field. This mode is used during large-angle slews and FHST and FGS occultations. It may also be entered when onboard attitude determinations (OBADs) fail, as guide star acquisitions will not be attempted.

Attitude is estimated in M2G mode through a combination of rates provided by the two gyros and the attitude derived from the cross product of the magnetic field model and the magnetic field measured by the MSS. The time derivative of the magnetic field is measured in the vehicle reference frame by the MSS. The data for this magnetic field change is filtered heavily before comparison to the expected value of the magnetic field derivative calculated from the magnetic field model. The difference between the measured and predicted values reveals the magnitude of pointing inaccuracies if the alignment of HST with the Earth's magnetic field is favorable for such comparisons.

M2G mode has the following sub-modes:

1. *Attitude Hold Mode*: This mode is used when gyro plane errors are expected to be small (e.g., after two successful onboard attitude determinations). The G_X axis is controlled by the MSS, while the gyro plane is controlled with the gyro rate information. This mode can be entered from the T2G mode after a successful OBAD.

2. *Maneuver Mode*: This mode is used to perform large-angle vehicle maneuvers. The G_X axis is controlled by the MSS, while the gyro plane is controlled with the gyro rate information in conjunction with additional information from the MSS. This mode can be entered only from the M2G attitude hold or M2G coarse attitude hold modes.

3. *Coarse Attitude Hold Mode*: This mode is used when significant gyro plane errors are expected (e.g., after an onboard attitude determination failure). The G_X axis is controlled by the MSS, while the gyro plane is controlled with the gyro rate information in conjunction with additional information from the MSS. This mode can be entered from the M2G maneuver mode or from the T2G mode after an unsuccessful OBAD.

4.3.2 Fixed-Head Star Trackers and Two Gyros (T2G)

The T2G mode uses two gyros in combination with one or more of the fixed-head star trackers to provide pointing control necessary to perform attitude determinations and to reduce the pointing uncertainty to less than 1 arc minute. HST has three FHSTs that are located at the aft end of the observatory. They are attached to the focal plane structure close to the gyroscopes. One FHST points along the **-V3** axis. The other two are tipped backwards and tilted relative to the **-V1** direction, pointing toward the rear of the observatory. The FHSTs have 8 x 8 degree fields of view and are sensitive to stars brighter than $m_V \sim 6$, with a typical centroiding accuracy of 10-15 arcseconds. The use of FHST information is required throughout the T2G mode.

Upon entering T2G mode from M2G mode, an FHST is used to lock onto the position of any star, and this information is fed into the control law to damp the vehicle rates about the G_X axis. After the rates have damped and while the FHST remains locked onto the star, a second FHST can be used to collect information about the star positions in its field of view. The star maps are compared to an onboard star catalog to determine the attitude of the observatory. This onboard attitude determination may be followed by a maneuver to correct the pointing, and a second OBAD is performed to ensure that the pointing has been refined sufficiently.

The rate damping in T2G mode following an M2G mode sequence is expected to take less than ~120 seconds. The attitude error following small (≈0.5 degree) maneuvers is expected to be ≤15 arcseconds. The attitude error following an extended period of attitude hold is expected to be ≤30 arcseconds.

T2G mode has three sub-modes:

1. *Rate Damping Mode*: This mode uses information from the FHSTs to damp the rates and to provide pointing stability in the G_X axis. It is the entry point into T2G mode from M2G mode. It is also the only mode that can be entered from zero gyro sunpoint (ZGSP) safemode.
2. *Attitude Hold Mode*: This mode determines and holds the observatory attitude after the rates have been damped. One or more OBADs with the FHSTs may occur while in this mode. It is the sole entry point into the F2G mode. It can be entered from the T2G rate damping

mode or from the F2G mode. It can also be re-entered from the T2G maneuver mode after a vehicle maneuver.

3. *Maneuver Mode*: This mode is used to perform the maneuvers required for attitude corrections following an OBAD in the T2G attitude hold mode. After the maneuver, control is returned to the T2G attitude hold mode.

4.3.3 Fine Guidance Sensors and Two Gyros (F2G)

The F2G mode uses information from the HST FGSs in combination with two gyros to provide the fine pointing control required for guide star acquisitions and science observations. Just before entering F2G mode, an FGS is used to find and track a star. Upon entering F2G mode, the FGS is used in coarse track mode to control the attitude along the G_X axis and dampen the rates remaining from the T2G activities. A second FGS then searches for a guide star, enters coarse track mode, and proceeds to fine lock. Once in fine lock, it provides information for the G_X axis. After the jitter is low enough, the first FGS transitions into fine lock and reduces the jitter even further so that the guide star acquisition and science observations can be performed.

The F2G mode has two sub-modes:

1. *F2G-CT*: This is the F2G coarse track mode. This mode is used to damp the gyro rates remaining from T2G mode in preparation for entry into F2G fine lock mode.

2. *F2G-FL*: This is the F2G fine lock mode. Science observations are obtained in this mode after the guide star acquisition is completed. The jitter in this mode is comparable to the jitter observed in three-gyro mode. Control in this mode is performed using the dominant (brighter) guide star.

An abort from either F2G sub-mode results in the attitude control system dropping back into T2G mode. From here, it may be necessary to drop into M2G mode if FHST visibility is insufficient to remain in T2G mode.

4.3.4 A Typical Sequence of Events for an Acquisition

The general sequence of events that must occur for an HST science observation to be made (slew, guide star acquisition, and science observation) are the same in three-gyro mode and two-gyro mode, but the implementation of these events is considerably different. Figure 4.2 depicts these events in graphical form. The sequence for both modes begins with a slew to the target.

In three-gyro mode, a short FHST update may sometimes be required between the end of the slew and the start of the guide star acquisition process. This update can use any FHST and can occur at any point before the acquisition. When the FGSs come out of occultation, the guide star acquisition occurs and is followed immediately by the science observation(s), which may include a target acquisition. The science observation can continue until the target is occulted. During occultation, the telescope pointing drifts by less than ~5 arcseconds. On subsequent orbits, a guide star re-acquisition occurs and is followed by another science observation.

In two-gyro mode, the slew is performed in M2G mode under the control of two gyros and the MSS. T2G mode is entered when an FHST becomes available, and the resulting M2G gyro rates are damped while the observatory waits for a second FHST to become available. Once this occurs, the FHSTs are used to locate stars for an onboard attitude determination and to correct the pointing, which may be off by as much as 10 degrees. (OBADs are indicated by the "map" blocks in Figure 4.2.) A second OBAD is required to check the correction, and this information is used to refine the pointing even further. While waiting for the FGSs to become unocculted, the FHSTs are used to stabilize the pointing. When an FGS is available, the guide star acquisition process commences and F2G mode is entered to reduce the pointing uncertainties and jitter even further. The science observation begins at the end of the guide star acquisition. During occultation the control system drops back to M2G mode, and the whole process, from M2G through F2G, must be repeated for the next orbit.

Figure 4.2: Typical Sequence of Events for an Observation

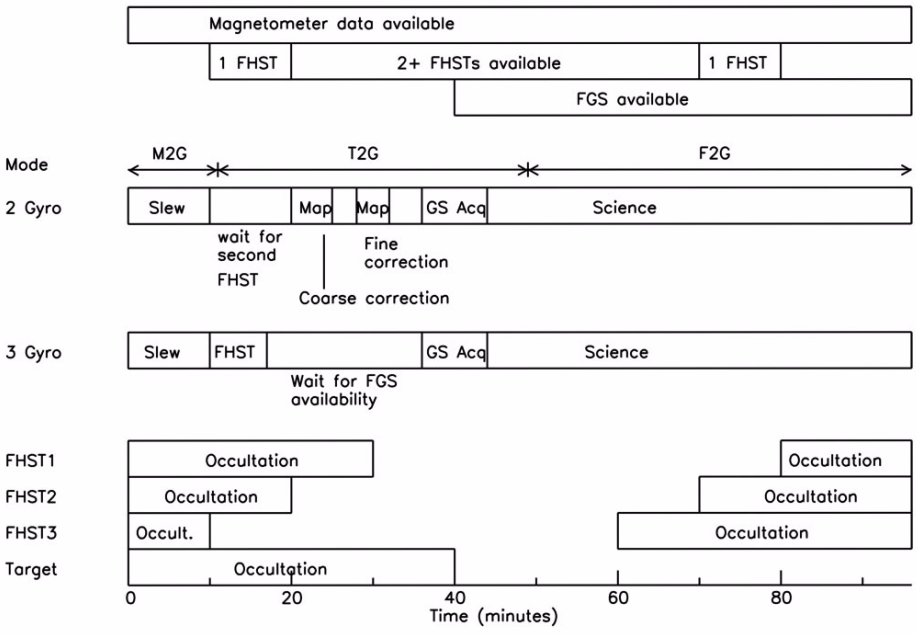

4.3.5 Gyro-only Pointing

Observing without the use of guide stars (gyro-only pointing) is occasionally allowed in three-gyro mode (see Section 3.2.3 of the *HST Primer*). In two-gyro mode, gyro-only pointing is not allowed for external science observations. It may still be used for external Earth-calibration exposures or internal calibration exposures.

4.4 Pointing Constraints

The need to use a sequence of MSS, FHSTs, and FGS observations to provide attitude control information for the G_X axis in two-gyro mode results in a set of pointing constraints that is more stringent than in three-gyro mode. The pointing uncertainty of as much as 10 degrees in M2G mode requires more stringent Sun-avoidance constraints. The need to have FHST coverage throughout T2G mode also results in reduced scheduling possibilities since multiple FHSTs must be unocculted by the Earth at the appropriate times. This latter constraint is the primary reason for the reduced schedulability of targets in directions ahead of the Sun (see Chapter 2). A summary of pointing constraints in both three-gyro mode and two-gyro mode is provided in Table 4.1.

Table 4.1: Pointing Constraints Summary

Pointing Constraint	Three-Gyro Mode	Two-Gyro Mode
Sun angle range allowed	50˚-180˚	60˚-180˚
Off-nominal roll angle allowed	5˚ for V1-Sun angle 50˚-90˚; increasing to 30˚ at V1-Sun angle = 178˚; unlimited at V1-Sun-angle = 178˚-180˚	5˚ for V1-Sun angle 60˚-115˚; increasing to 20˚ at V1-Sun angle = 179˚; unlimited at V1-Sun-angle = 179˚-180˚
V1 Moon constraint (FGS HV on)	>9.5˚	Same as three-gyro mode
Earth avoidance (FGS guiding, dark limb)	>6˚	Same as three-gyro mode
Earth avoidance (Science obs, dark limb)	>6˚	Same as three-gyro mode
Earth avoidance (FGS guiding, bright limb)	>13.5˚	Same as three-gyro mode
Earth avoidance (Science obs, bright limb)	>20˚	Same as three-gyro mode
SAA avoidance	Instrument dependent	Same as three-gyro mode

CHAPTER 5:

Guiding and Jitter

In this chapter . . .

5.1 Guiding

The general procedures for acquiring guide stars in preparation for science observations are outlined in the *Slewing and Pointing* chapter of this Handbook. Here, we concentrate on a few key issues that are relevant for guiding while science observations are taking place.

5.1.1 Guide Star Acquisitions

Guide star acquisitions in two-gyro mode take the same amount of time as those routinely performed in three-gyro mode (~6 minutes). Unlike three-gyro mode, however, the pointing errors accumulated during occultations by the Earth in two-gyro mode are expected to be sufficiently large to prevent the types of guide star re-acquisitions that are currently performed in three-gyro mode. Therefore, full guide star acquisitions are performed every orbit in two-gyro mode.

Single guide star acquisitions have sometimes been necessary when two suitable guide stars could not be acquired by the FGSs. While this type of acquisition is possible in three-gyro mode, single guide star acquisitions are not allowed in two-gyro mode. If a pair of suitable guide stars cannot be acquired in two-gyro mode during the guide star acquisition, the pointing control system will drop into a coarser pointing mode (see Section 4.3).

Table 5.1 summarizes some of the relevant guide star acquisition differences between three-gyro and two-gyro mode.

Table 5.1: Guide Star Acquisitions

Activity	Three-Gyro Mode	Two-Gyro Mode
Guide star acquisition (initial orbit in visit)	~6 min	~6 min
Guide star acquisition (orbits following initial orbit in visit)	~5 min (re-acquisition)	~6 min
Single guide star acquisition	Allowed	Not Allowed
Dual guide star acquisition with only 1 star successfully acquired	Observation proceeds successfully in many cases	Acquisition fails; revert to T2G or M2G mode

5.1.2 Guide Star Magnitudes

Unlike three-gyro mode, pointing performance and maintenance of guide star lock in two-gyro mode depend on the magnitudes of the guide stars chosen. Figure 5.1 shows a histogram of the magnitudes of all guide stars used by HST from January 2000 through August 2004. The average guide star magnitude in this time period was $m_V = 12.1$, with a median magnitude of $m_V = 12.3$. These estimates include magnitudes for both dominant and secondary guide stars (when available). Some guide stars were used multiple times. On average, 25% of the guide stars were brighter than $m_V = 11.3$, and 25% were fainter than $m_V = 13.1$. Less than 1% of the guide stars used were fainter than $m_V \geq 14.0$. Chapter 7 contains additional information about the brightness distribution of the guide stars for each FGS in this time period.

Figure 5.1: HST Guide Star Magnitudes (Jan. 2000 - Aug. 2004)

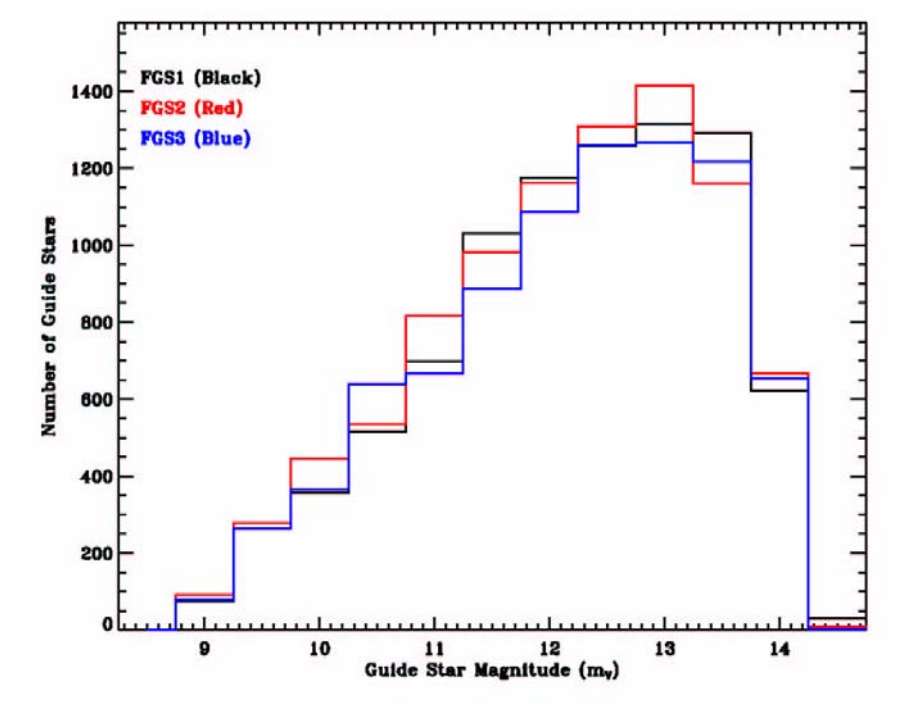

5.1.3 Guiding Performance

On-orbit tests in February 2005 showed that the guiding performance in two-gyro mode (F2G-FL) is similar to the guiding performance in three-gyro mode. Additional tests are planned for August 2005 to quantify the guiding performance more accurately so that updates will be available in time for Cycle 15 Phase II proposal preparations.

An important consideration for faint ($m_V \geq 14.0$) guide stars is the possibility that HST may lose lock under special circumstances. The primary concern is that the FGSs used to guide are also providing pointing information to the attitude control system. Loss of lock is expected to occur only if substantial disturbances occur while guiding on faint stars. The gyro pair available in two-gyro mode will affect the probability of loss of lock since the various types of disturbances change the pointing in preferred directions. Simulations of the jitter caused by different disturbances (see below) and the past history of guide star magnitudes in Chapter 7 indicate that loss of lock will occur infrequently, and perhaps only if multiple disturbances are present simultaneously. If loss of lock does occur, science data collection will cease, and it may or may not be possible to resume science observations during the impacted visit. Loss of lock results in the pointing control dropping into T2G mode (if FHST visibility is available) or even into M2G mode (if no FHSTs are available at the time of loss of lock).

5.2 Jitter Overview

5.2.1 Jitter Description

The HST gyroscopes are oriented with respect to each other so that three functioning gyroscopes can be used to provide three-axis stability for the telescope. Small high-frequency motions of the observatory caused by noise in the gyros and fine guidance sensors, mechanical vibrations, disturbances in the pointing induced by thermal and mechanical effects, gravity gradients across the observatory, and atmospheric drag introduce small changes in the telescope pointing while it is in fine guiding mode obtaining science data. As a result, the HST pointing is constantly changing over very small angular scales that are set by the pointing control law in the attitude control system.

The magnitude and shape of telescope jitter in the **V2**-**V3** plane[1] is expected to be only slightly different in two-gyro mode than in three-gyro mode. Typical root-mean-square (RMS) pointing jitter of less than ~5 mas over 60-second intervals is currently achieved in three-gyro mode. For two-gyro mode, a comparable jitter magnitude is observed (see Table 1.1). We provide more information about the sources, frequencies, and magnitude of the jitter predicted by simulations below.

5.2.2 Jitter Orientation

Plotted on the plane of the sky (the **V2-V3** observatory plane) as a function of time, the present three-gyro telescope pointing while guiding with the fine-guidance sensors is described by a nearly circular distribution of points with a typical RMS pointing jitter of <5 mas. Reducing the number of gyros from three to two results in a loss of gyro information for one axis. With two gyros, the circular jitter distribution becomes an ellipse since there is less precise control in the direction orthogonal to the plane defined by the two functioning gyros. As of the writing of this document, Gyros #1 and #2 are operating, and Gyros #6 and #4 are functional but turned off. Table 5.2 lists the angle of the G_X axis on the plane of the sky for each possible pair of remaining gyros. The component of jitter about the G_X axis in each direction is also listed. For reference, Figure 5.2 contains a map of the HST field of view showing the relative positions of the science instruments projected onto the **V2**-**V3** plane.

1. The **V1**, **V2**, and **V3** coordinate system is sometimes referred to in other HST documentation as the **U1**, **U2**, **U3** coordinate system, in which **V1** = **U1**, **V2** = **-U2**, and **V3** = **-U3** (see Figure 5.2). The plane of the sky lies in the **V2**-**V3** plane. Observatory roll occurs about the **V1** axis; pitch occurs about the **V2** axis; and yaw occurs about the **V3** axis.

Table 5.2: Two-Gyro Jitter Ellipse Orientations

Gyro Set	Component of G_X			Angle of G_X Axis on Plane of Sky[1]
	(V1 Direction)	(V2 Direction)	(V3 Direction)	
1 & 2	0.0	1.0	0.0	0.0°
1 & 4	0.5303	-0.7820	-0.3275	-22.7°
1 & 6	-0.5303	-0.7820	0.3275	22.7°
2 & 4	-0.8005	0.3387	-0.4994	55.6°
2 & 6	0.8005	0.3387	0.4994	-55.6°
4 & 6	-0.6678	0.0	-0.7443	90.0°

1. Angle is measured from the **V3** axis counterclockwise in the **V2-V3** (sky) plane (see Figure 5.2).

Figure 5.2: HST Field of View Following SM3B

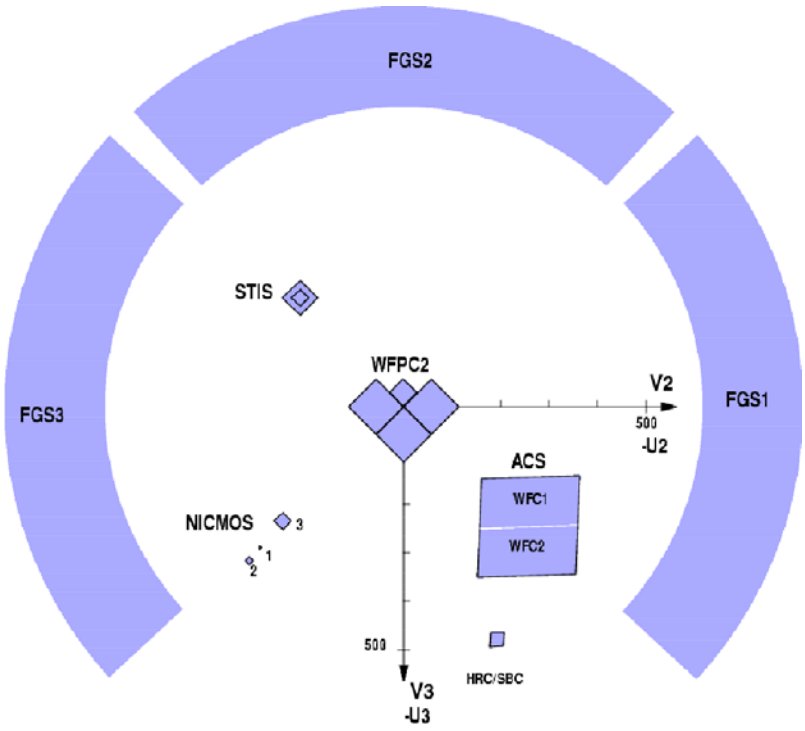

5.2.3 Sources of Jitter

There are numerous sources of jitter in the HST pointing, but many of these sources have little impact on the total jitter budget. The dominant sources include thermal gradients across the solar arrays, high gain antenna

(HGA) gimbal articulations, occasional disturbances about the **V2** axis believed to be caused by rotations of the SSM equipment shelf, reaction wheel zero-speed crossings, rate gyro noise, and FGS photomultiplier tube (PMT) noise. Very small contributions (<2 mas) arise from ACS filter wheel motions and SSM thermal gradients.

In two-gyro mode, jitter contributions from the combination of rate gyro noise and FGS PMT noise are slightly larger than the rate gyro noise alone in three-gyro mode. The noise introduced into the attitude control law by the Fine Guidance Sensors used to provide pointing control information about the G_X axis is particularly important when fainter guide stars are used because of reduced signal-to-noise in the FGS measurements. Information about the jitter caused by rate gyro noise and FGS PMT noise can be found in Chapter 6.

Approximate values for the jitter introduced by various sources are listed in Table 5.3. These values are expected to be conservative (generous) estimates of the jitter based upon simulations used to predict the response of HST to disturbances encountered on-orbit. Descriptions of the primary sources of jitter in this table can be found in Section 5.3.

Table 5.3: Sources of Jitter in the Two-Gyro F2G-FL Jitter Budget

Jitter Source		Jitter (mas, 60-sec RMS)	Comment
Solar Array (SA3) Thermal Gradients		8.92	Frequent
V2 Disturbances		4.13	Frequent
High Gain Antenna (HGA) Gimbal Articulations	Low-rate TDRSS tracking	3.35	Usually present
	High-rate slews	8.02	Intermittent
Reaction Wheel Zero-Speed Crossings	Hot attitude	2.50	Frequent
	Cold attitude	6.00	
FGS PMT + Rate Gyro Noise		3.90	Always present
ACS Filter Wheels		<2.0	Minimal contribution
SSM Thermal Gradients		1.59	Minimal contribution

5.2.4 Jitter Frequencies

The HST pointing is most susceptible to disturbances with frequencies between 0.01 and 0.5 Hz, or periods between 100 and 2 seconds. Higher frequency disturbances damp very quickly. Some sources of jitter (aero and gravity torques, for example) have very low frequencies. The FGS and gyros provide pointing information at a rate of 40 Hz. The pointing control

law implemented in the F2G-FL mode has a closed-loop post-filtered bandwidth of ~1 Hz for the entire system, including the G_X axis and gyro plane. Therefore, it is possible to observe and correct for many sources of jitter, even in two-gyro mode.

5.3 Disturbances and Primary Sources of Jitter

There are several types of disturbances that contribute to the jitter expected in two-gyro mode. Below we discuss the most important disturbances listed in Table 5.3.

5.3.1 Solar Array (SA3) Disturbances

Thermal gradients across the third set of HST solar arrays, which were installed during SM3B, lead to several different motions of the solar arrays as they release accumulated stresses. The most important motion is an in-plane bending occurring at a frequency of ~1 Hz. The solar array disturbances occur irregularly; they are not traceable to terminator crossings but are related to the thermal changes caused by the motion of HST around the Earth.

SA3 disturbances last 1-2 seconds and have a variety of amplitudes. Trending of past SA3 events by the HST PCS Group yields the expected frequency of disturbances summarized in Table 5.4. Like the V2 disturbances, the SA3 disturbances are not likely to cause significant data quality degradation unless the event occurs during a short (<10 second) science exposure. Both two-gyro and three-gyro observations are susceptible to these events.

The simulations conducted to date indicate that loss of lock may be an issue in two-gyro mode if SA3 disturbances with amplitudes greater than ~100 mas are encountered. This can be exacerbated if the SA3 disturbance occurs at the same time as disturbances cause by other sources (e.g., high gain antenna gimbal articulations). Loss of lock resulting from SA3 disturbances is most problematic for gyro combination 4-6 (the G_X axis has a significant component in the **V3** direction) and least problematic for gyro combination 1-2 (the G_X axis is purely in the **V2** direction). The probability of losing lock during an SA3 disturbance in two-gyro mode is higher for fainter guide stars. SA3 disturbances with amplitudes greater than ~300 mas will likely cause loss of lock for any gyro pair with guide star magnitudes $m_V > 14$. Even for bright guide stars (e.g., $m_V < 10$), loss of lock may still occur for gyro pairs 2-4, 2-6, and 4-6 if the SA3 disturbance has an amplitude greater than ~270 mas. Such events are relatively rare (~1 every 20 days). Combining the expected sensitivity of the different gyro pairs to loss of lock, past guide star magnitude distributions, and the SA3

disturbance frequencies in Table 5.4, the HST PCS Group predicts <1 loss of lock per day in two-gyro mode.

Table 5.4: SA3 Disturbance Frequency

Disturbance (mas)	Events/day
43.4	11
80.1	3.32
117.6	1.62
155.9	0.62
194.6	0.23
232.4	0.1
271.4	0.05
310.5	0.02
348.1	<0.01
384.5	<0.01

5.3.2 V2 Disturbances

V2 disturbances are brief (less than ~ 1 second) impulsive disturbances believed to be caused by the rapid motion of the Support Systems Module (SSM) Equipment Shelf about the **V2** axis. The motion of the shelf appears to be caused by the release of stresses accumulated in the mechanical structure of the shelf over time. The movement of the shelf itself does not correspond to a movement of the telescope, but the shelf motion does induce a subsequent telescope pointing change.

The HST gyros and FHSTs are mounted to the equipment shelf. When the shelf moves, the gyros sense the motion, and the control law reacts to the perceived motion of the telescope by commanding the reaction wheels to correct for the motion. The FGSs, which are guiding on stars, detect this commanded motion and feed information into the attitude control loop to move the boresight to the proper position necessary to return the stars to their original positions. After this corrective motion, the telescope is once again pointed properly, but the equipment shelf remains rotated relative to its position before the V2 disturbance.

V2 disturbances typically occur in groups of ~5 events, with spacings of a few minutes. The peak-to-peak excursions of the disturbances range from ~25 mas to ~200 mas. The most probable events are those with 50-55 mas amplitudes. Table 5.5 lists the number of expected V2 disturbances per day

as a function of amplitude. V2 disturbances are more common for large off-nominal roll angles.

Table 5.5: V2 Disturbance Frequency

Disturbance (mas)	Events/day
55	10.0
60	7.6
65	4.2
70	2.6
75	1.7
80	1.3
85	0.98
90	0.76
95	0.63
100	0.49
105	0.36
110	0.25
115	0.17
120	0.12
200	<0.01

HST is susceptible to V2 disturbances in two-gyro mode as well as three-gyro mode. However, the sensitivity to these disturbances in two-gyro mode will depend strongly on which pair of gyros is operating because the disturbances occur only about the **V2** axis. Gyro combination 1-2 has a G_X axis oriented along the **V2** direction. Therefore, the gyros cannot detect a rotation of the equipment shelf about the V2 axis. As a result, no command would be given to induce telescope motion, and no subsequent command would need to be issued to correct the telescope pointing. Other gyro combinations can sense the shelf rotation; combination 4-6 is the most sensitive since the **V2** axis is completely within the gyro plane. In this case, the behavior of the telescope pointing and the resulting jitter induced by the disturbance would be similar to that encountered in three-gyro mode.

Using the past history of V2 disturbance amplitudes measured on-orbit, the simulations predict that V2 disturbances will not cause loss of guide star lock, even for faint guide stars. These disturbances will not significantly affect data quality of long exposures because the disturbance

duration is brief. However, V2 disturbances could severely degrade the quality of short (<10 second) exposures if the exposures occur during the brief disturbance intervals; this is rather unlikely in most cases, but observers should be aware of this possibility. This cautionary note applies for observations in both two-gyro and three-gyro mode.

5.3.3 High Gain Antenna Motions

HST has two high gain antennae (HGA) that are used to provide communications with the Tracking and Data Relay Satellite System (TDRSS). The antennae are used to receive commanding instructions and to return engineering and science data. Each steerable HGA sits at the end of a boom extending along the **V3** axis and is gimbaled to provide tracking capability as HST orbits the Earth. The gimbal articulations required to position the two HST antennae properly for communications with the TDRSS satellites contribute to the HST jitter budget in two-gyro mode. The magnitude of the jitter depends upon the antenna tracking mode.

Low-rate tracking during communication with the TRDSS satellites or during preparations for communication contributes about 3.0-3.5 mas of jitter (RMS value over a 60 second time interval). The jitter induced by this "ephemeris tracking" is caused primarily by translational bending of the booms along the **V1** and **V2** axes. It occurs almost constantly since the antennae are often in this tracking mode.

High-rate tracking can also introduce jitter. There are two general types of high-rate tracking - "hardware splines" and "jitter splines". Hardware splines occur at a tracking rate near the hardware limit of 30 degrees per minute. They occur roughly 25 times per week for periods of 5-16 minutes, and they are used only during vehicle slews. They are not currently used during guiding. Jitter splines are more common (~60 times per week). About half have tracking rates of <2 degrees per minute, and half have rates of 6-12 degrees per minute. They range in duration from about 10 minutes to 8 hours, with an average duration of about 1.5 hours. The total fraction of time spent in jitter spline mode is about 50%. The simulations described below include the worst case high-rate tracking jitter expected - about 8 mas RMS averaged over a 60 second time interval.

5.4 HSTSIM Jitter Simulations

HSTSIM is a high-fidelity, non-linear time domain HST pointing performance simulator developed and maintained by the Pointing Control Systems Group at Lockheed Martin Technical Operations (LMTO) Company. It includes realistic models for the HST hardware (FGS, FHSTs, gyroscopes, etc.) as well as models of orbital dynamics, the Earth's

magnetic field, and sources of attitude disturbances (e.g., high gain antenna moves, V2 and SA3 disturbances, and aerodynamic and gravity gradients). The information in this section is based on the disturbance data analysis and simulations conducted in the summer of 2004 by Brian Clapp and the PCS Group at LMTO.

5.4.1 Integrated Jitter Predictions

HSTSIM models were run for the full range of possible gyro pairs in two-gyro mode. A three-gyro model was also constructed for the currently operating 1-2-4 gyro set. The HSTSIM jitter predictions for three-gyro guiding mode are shown in Figure 5.3, and the predictions for the F2G-FL mode with the 1-4 gyro combination are shown in Figure 5.4. These models incorporate sample disturbances of the type described above, including an SA3 disturbance with an amplitude of 80 mas, thirteen V2 disturbances with amplitudes of 60-120 mas, and HGA tracking disturbances. The timelines shown are not meant to mimic a particular on-orbit combination of disturbance events, but rather are designed to explore the sensitivity of the possible gyro combinations to a variety of different types of disturbances. Clearly, multiple disturbances can be combined to produce larger amounts of jitter.

Figure 5.3: Three-Gyro Jitter Simulation Example with Disturbances

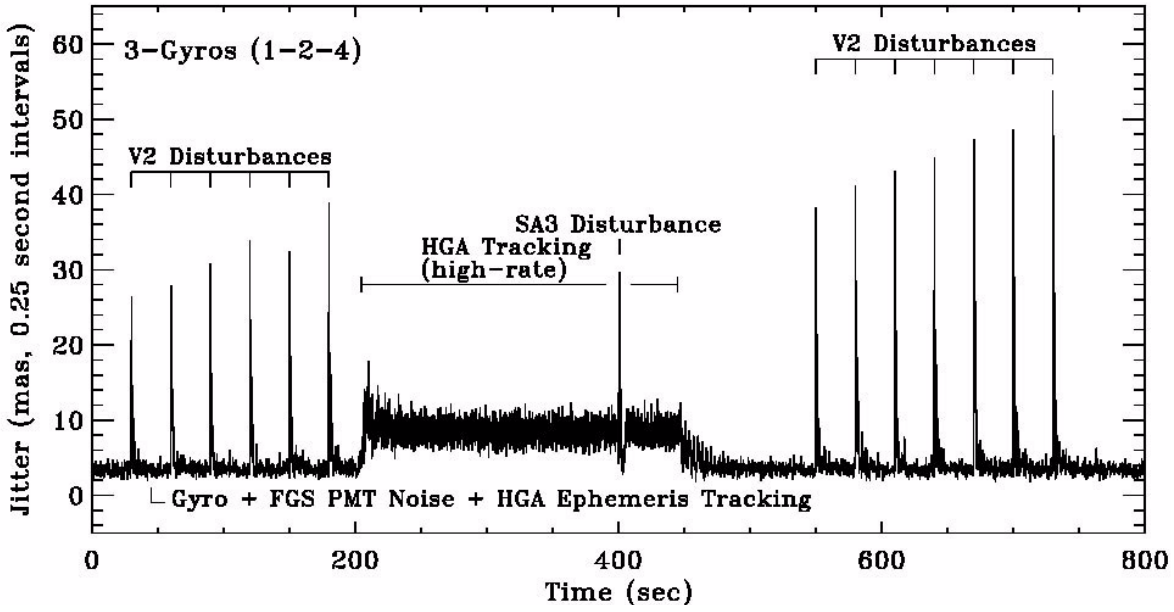

Figure 5.4: F2G-FL Two-Gyro Jitter Simulation Example with Disturbances

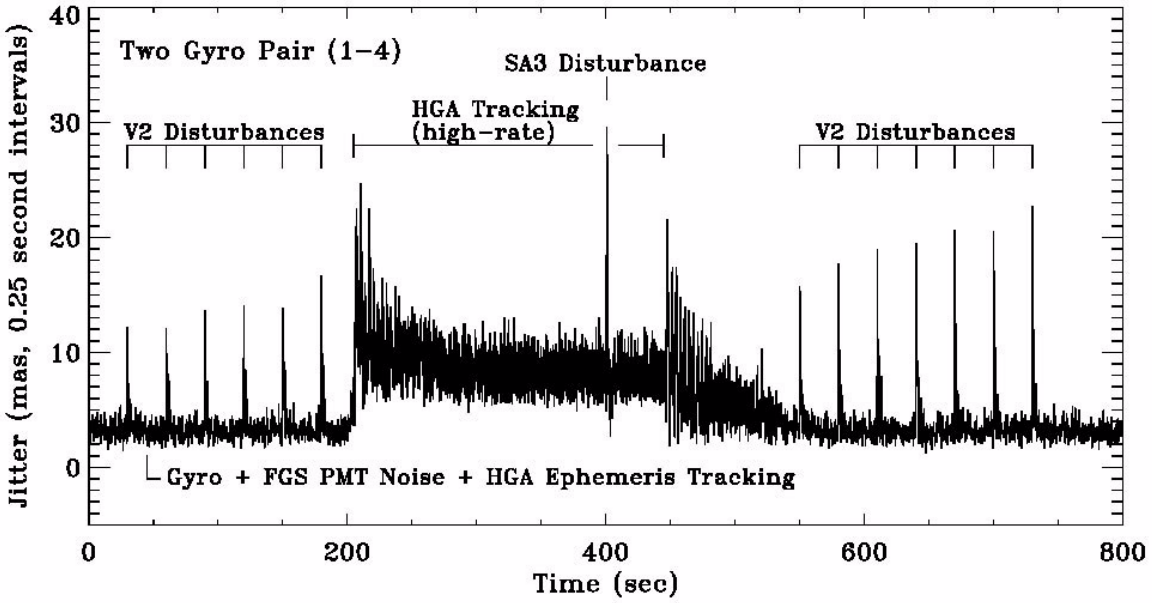

Sample jitter ellipses in the **V2**-**V3** plane are shown in Figure 5.5 for the 1-4 and 2-6 gyro pairs. The data in the upper middle panel corresponds to the jitter time series shown in Figure 5.4 for gyro pair 1-4 with a 13^{th} magnitude guide star. The large excursions caused by V2 disturbances are evident in all six panels. Note the slight increase in the jitter as the guide star magnitude increases. The increase in this jitter ellipse axis results from the increased FGS PMT noise in the simulations with the fainter guide stars. The points in these panels have been binned into 0.25 second jitter averages to make it easier to see these effects. Data from the full 800 second simulations are shown.

Figure 5.5: Jitter Ellipses for Two Possible Pairs of Gyros

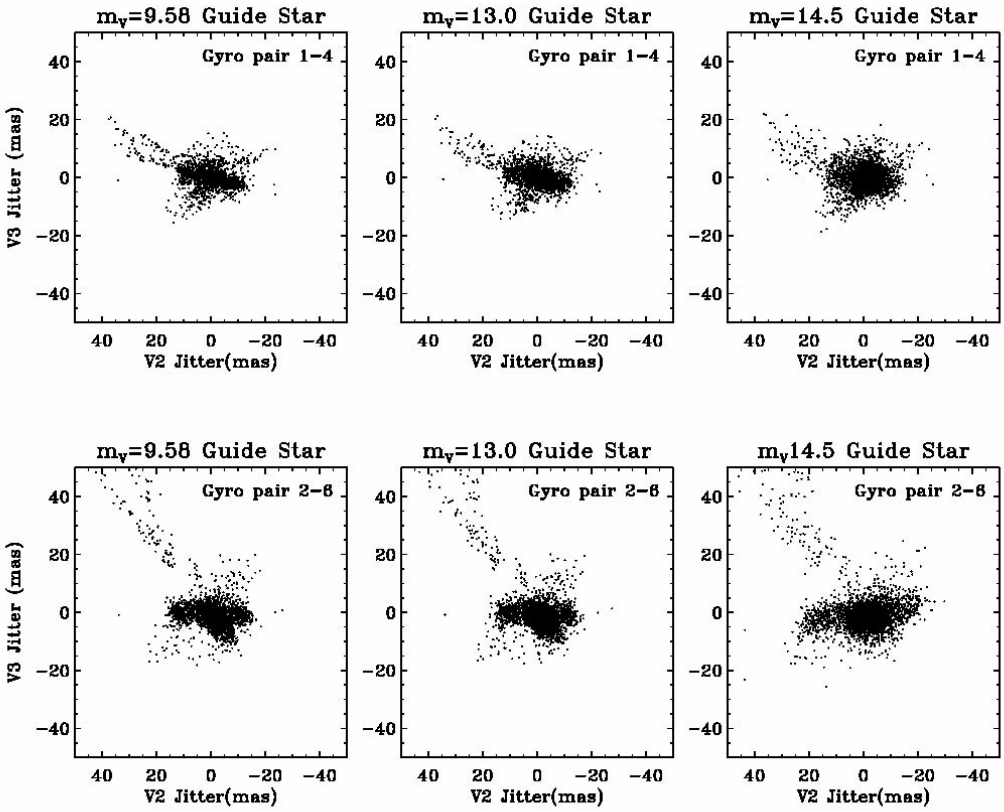

Table 5.6 summarizes the expected jitter in two-gyro mode based upon the HSTSIM predictions. For each possible two-gyro combination and three different FGS guide star magnitudes, the table lists the maximum root-mean-square (RMS) jitter measured in any 60 second interval during the F2G-FL portion of the simulations. The assumptions used in these predictions are the same as those described for the simulation data above. The corresponding values for three-gyro mode are listed at the bottom of the table. Note that these are the maximum values expected; typical jitter values for times between SA3 and V2 disturbances will be considerably less.

Table 5.6: Two-Gyro and Three-Gyro Jitter Predictions (Including Disturbances)

Gyro Set	Angle of G_X Axis on Plane of Sky[1]	Maximum Boresight Jitter (mas, 60-second RMS) [2]		
		m_V = 9.58	m_V = 13.0	m_V = 14.5
Two-Gyro F2G-FL Results				
1-2	0.0	9.55	9.76	10.40
1-4	-22.7	10.65	10.86	11.65
1-6	22.7	11.72	11.91	13.06
2-4	55.6	12.20	12.30	15.97
2-6	-55.6	12.39	12.47	17.41
4-6	90.0	12.26	12.49	18.93[3]
Three-Gyro Results				
1-2-4	N/A	9.73	9.73	9.75

1. Angle is measured from the **V3** axis counterclockwise in the **V2-V3** (sky) plane (see Figure 5.2).
2. These values are the maximum jitter encountered during any 60 second interval in the F2G-FL portion of the simulation.
3. Loss of lock occurred during SA3 disturbance concurrent with high-rate HGA track.

CHAPTER 6:

Quiescent F2G-FL Jitter Predictions

In this chapter. . .

6.1 HSTSIM Quiescent Jitter Predictions

Estimates of the magnitude of the jitter in F2G-FL mode caused by rate gyro noise and FGS photomultiplier tube (PMT) noise are listed in Table 6.1 for various combinations of guide star magnitudes (m_v = 9.58, 13.0, and 14.5) and possible gyro pairs. The jitter values listed are the maximum values expected for a 60 second exposure; they are only slightly larger than those predicted for the gyro noise in three-gyro mode. These "quiescent" simulations include only the jitter contributions from these two sources and do not include more prominent contributions from the on-orbit disturbances that contribute to the overall jitter budget discussed in Chapter 5.

Sample two-gyro jitter ellipses in the **V2**-**V3** plane caused by rate gyro noise and FGS PMT noise are shown in Figure 6.1 for the 1-4 and 2-6 gyro pairs. No disturbances are included in these simulations; see Chapter 5 for a similar figure that includes disturbances. In the quiescent simulations, the shape of the jitter in the **V2**-**V3** plane depends strongly on the magnitude of the guide star used by the FGS to measure motions about the G_X axis. For bright guide stars, the FGS measures motions about the G_X axis very precisely, and the jitter is elongated in a direction corresponding to measurement of motions by the gyros (i.e., most of the jitter is contributed by gyro noise rather than FGS PMT noise – see the left panels in the figure). For faint guide stars, the jitter shape becomes more circular, with an increase in the magnitude of the jitter in the direction corresponding to

the measurement of motions about the G_X axis (i.e., PMT noise becomes more prominent – see right panels in the figure).

Table 6.1: Quiescent Two-Gyro Jitter Predictions (No Disturbances)

Gyro Pair	Angle of G_X Axis on Plane of Sky[1]	Maximum F2G-FL Boresight Jitter (mas, 60-second RMS) [2]		
		m_V = 9.58	m_V = 13.0	m_V = 14.5
1-2	0.0	1.17	1.63	3.20
1-4	-22.7	1.28	1.78	3.42
1-6	22.7	1.29	1.85	3.42
2-4	55.6	2.70	2.88	3.89
2-6	-55.6	2.62	2.90	3.93
4-6	90.0	1.48	2.03	3.38

1. Angle is measured from the **V3** axis counterclockwise in the **V2-V3** (sky) plane (see Figure 5.2).
2. These values reflect only the jitter caused by rate gyro noise and FGS PMT noise.

Figure 6.1: Jitter Ellipses Resulting from Rate Gyro Noise and FGS PMT

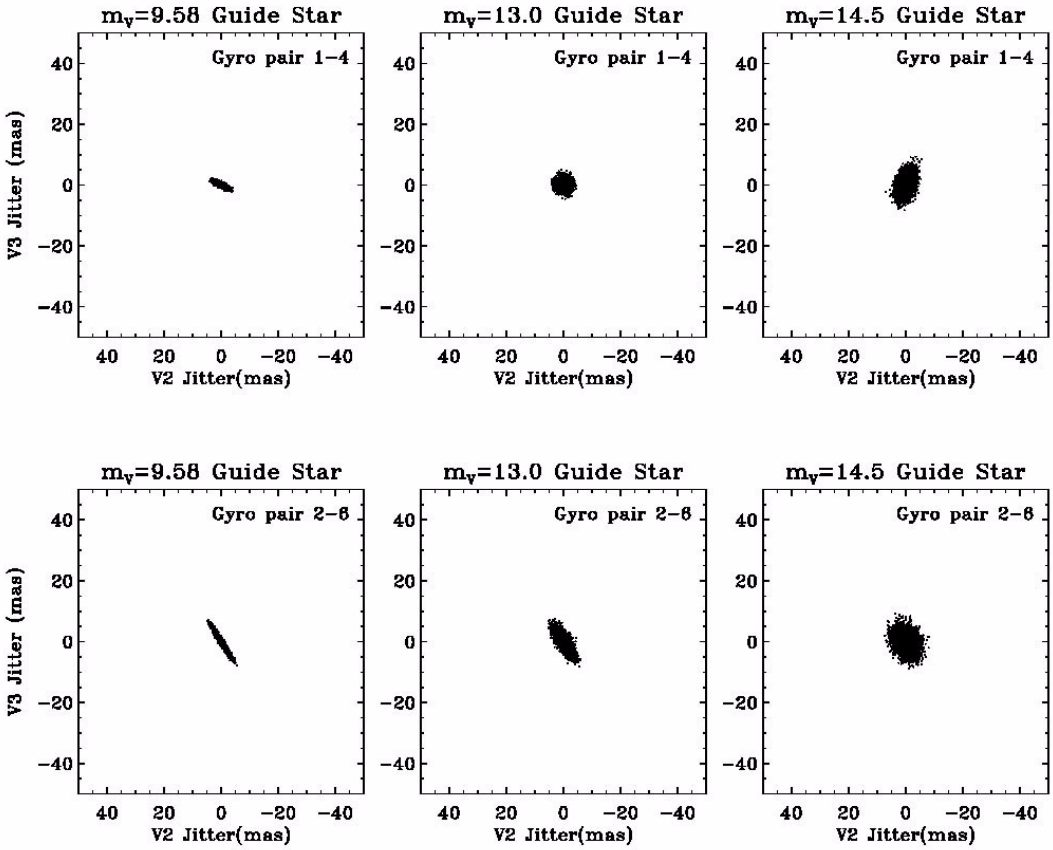

CHAPTER 7:

Guide Star Magnitudes

In this chapter. . .

7.1 Guide Star Magnitude Tables

The following tables contain information about the brightness distributions of guide stars in the three Fine Guidance Sensors from January 2000 through August 2004. Both dominant and secondary guide stars are included. A small number of these guide stars resulted in failed acquisitions.

The magnitude distributions are based upon the predicted (catalog) magnitudes of the guide stars. The typical uncertainty in the magnitudes is 0.3-0.5 mag. Although it is possible to use guide stars fainter than $m_V = 14$, few such instances occur since brighter guide stars can usually be found.

Table 7.1: HST FGS1r Guide Star Brightness Distribution (January 2000 - August 2004)

m_V	Percentage of Guide Stars Brighter than Listed Magnitude (8652 total, 5833 unique)				
	Y2000	**Y2001**	**Y2002**	**Y2003**	**Y2004**
9.5	1.2	2.0	2.5	1.6	1.9
10.0	3.5	6.8	8.6	6.0	5.9
10.5	6.3	13.3	15.0	10.8	10.5
11.0	11.0	21.4	22.4	17.8	17.1
11.5	17.7	34.2	36.5	25.5	27.6
12.0	26.4	47.7	52.0	43.1	39.9
12.5	39.2	61.1	64.7	57.1	54.6
13.0	55.9	74.5	76.5	75.0	68.7
13.5	75.8	88.1	88.0	87.7	84.1
14.0	99.8	99.7	99.5	99.3	99.9
14.5	100.0	100.0	100.0	100.0	100.0
Total	1652	1751	1645	2004	1600

Table 7.2: HST FGS2 Guide Star Brightness Distribution (January 2000 - August 2004)

m_V	Percentage of Guide Stars Brighter than Listed Magnitude (8876 total, 6003 unique)				
	Y2000	**Y2001**	**Y2002**	**Y2003**	**Y2004**
9.5	1.1	3.4	2.4	2.0	1.8
10.0	4.2	8.6	7.4	5.9	5.2
10.5	8.2	15.5	13.8	11.6	10.5
11.0	12.7	25.0	23.5	19.1	17.3
11.5	18.4	34.5	35.4	28.9	24.8
12.0	27.5	49.4	49.8	42.9	38.0
12.5	41.9	63.3	64.2	54.1	52.4
13.0	58.3	77.2	76.9	71.5	68.7
13.5	76.7	89.9	87.4	84.4	84.5
14.0	99.6	100.0	99.9	99.7	99.9
14.5	100.0	100.0	100.0	100.0	100.0
Total	1135	1983	1886	2060	1812

Table 7.3: HST FGS3 Guide Star Brightness Distribution (January 2000 - August 2004)

m_V	Percentage of Guide Stars Brighter than Listed Magnitude (8387 total, 5744 unique)				
	Y2000	**Y2001**	**Y2002**	**Y2003**	**Y2004**
9.5	1.2	2.3	2.8	2.5	5.0
10.0	3.3	7.2	7.5	6.1	6.8
10.5	7.2	12.8	13.7	11.4	12.6
11.0	11.7	20.8	23.6	24.8	16.6
11.5	18.2	31.7	33.5	34.4	25.4
12.0	27.9	46.2	48.3	46.6	35.9
12.5	41.7	59.9	62.1	61.5	47.3
13.0	58.7	75.8	76.5	75.3	64.5
13.5	76.1	89.4	87.2	88.6	80.6
14.0	100.0	99.9	99.6	99.7	99.9
14.5	100.0	100.0	100.0	100.0	100.0
Total	2050	2013	1769	1792	763

Glossary

The following terms and acronyms are used in this Handbook.

ACS: Advanced Camera for Surveys

ACS / HRC: ACS High-Resolution Channel

ACS / SBC: ACS Solar-Blind Channel

ACS / WFC: ACS Wide-Field Channel

APT: Astronomer's Proposal Tools

CP: Call for Proposals

CCD: Charge-coupled device

CVZ: Continuous viewing zone

ETC: Exposure time calculator.

F2G: Fine guidance sensor / two-gyro (mode)

FAQ: Frequently asked questions

FGS: Fine Guidance Sensor

FGS1r: Fine Guidance Sensor replacement for FGS1 (in SM2)

FRB: Failure Review Board

FHST: Fixed-head star tracker

GO: Guest Observer

HDF: Hubble Deep Field

HGA: High gain antenna

Help Desk: Facility for getting help on HST related topics via email. help@stsci.edu.

HST: Hubble Space Telescope

HUDF: Hubble Ultra-Deep Field

HV: High voltage

NICMOS: Near-Infrared Camera and Multi-Object Spectrograph

mas: milli-arcseconds

M2G: MSS / two-gyro (mode)

MSS: Magnetic Sensing System

OBAD: Onboard attitude determination

OTA: Optical Telescope Assembly

PCS: Pointing control system

Phase I proposal: A proposal for observing time on HST

Phase II program: An approved HST program; includes precise detail of how program is to be executed

PI: Principal Investigator

PMT: Photomultiplier tube

POS: POSitional (mode of FGS operation)

PSF: Point spread function

RA: Right Ascension (also denoted by "α")

RMS: Root-mean-square

RSU: Rate sensing unit

SA3: Solar arrays (third set installed during SM3B)

SAA: South Atlantic anomaly

SAZ: Solar avoidance zone

SM: Servicing Mission (as in SM1, SM2, SM3A, SM3B)

SMOV: Servicing Mission Observatory Verification

SNAP: SNAPshot (type of HST observation)

SNR: Signal-to-noise ratio

SSM: Support Systems Module

STIS: Space Telescope Imaging Spectrograph

STS: Space Transport System (Space Shuttle)

STScI: Space Telescope Science Institute

T2G: FHST / two-gyro (mode)

TAC: Time Allocation Committee

TDRSS: Tracking and Data Relay Satellite System

TGS: Two-Gyro Science

TOO: Target of opportunity

TRANS: TRANSfer (mode of FGS operation)

URL: Uniform resource locator

WFPC2: Wide Field Planetary Camera-2

WWW: World Wide Web

ZGSP: Zero-gyro sunpoint (safemode)

Index

V